Article

SOURCE DATA | TRANSPARENT PROCESS

THE EMBO JOURNAL

Synaptic activity controls localization and function of CtBP1 via binding to Bassoon and Piccolo

Daniela Ivanova[1,2], Anika Dirks[1], Carolina Montenegro-Venegas[1], Cornelia Schöne[1,†], Wilko D Altrock[1,3], Claudia Marini[1], Renato Frischknecht[1,3], Denny Schanze[4], Martin Zenker[4], Eckart D Gundelfinger[1,3,5,*] & Anna Fejtova[1,2,3,**]

Abstract

Persistent experience-driven adaptation of brain function is associated with alterations in gene expression patterns, resulting in structural and functional neuronal remodeling. How synaptic activity—in particular presynaptic performance—is coupled to gene expression in nucleus remains incompletely understood. Here, we report on a role of CtBP1, a transcriptional co-repressor enriched in presynapses and nuclei, in the activity-driven reconfiguration of gene expression in neurons. We demonstrate that presynaptic and nuclear pools of CtBP1 are interconnected and that both synaptic retention and shuttling of CtBP1 between cytoplasm and nucleus are co-regulated by neuronal activity. Finally, we show that CtBP1 is targeted and/or anchored to presynapses by direct interaction with the active zone scaffolding proteins Bassoon and Piccolo. This association is regulated by neuronal activity via modulation of cellular NAD/NADH levels and restrains the size of the CtBP1 pool available for nuclear import, thus contributing to the control of activity-dependent gene expression. Our combined results reveal a mechanism for coupling activity-induced molecular rearrangements in the presynapse with reconfiguration of neuronal gene expression.

Keywords cellular NAD/NADH balance; neuronal activity-regulated gene expression; neuronal plasticity; presynapse-to-nucleus signaling; synapto-nuclear shuttling

Subject Categories Neuroscience

DOI 10.15252/embj.201488796 | Received 25 April 2014 | Revised 7 January 2015 | Accepted 8 January 2015 | Published online 4 February 2015

The EMBO Journal (2015) 34: 1056–1077

See also: **DO Kravchick & BA Jordan** (April 2015)

Introduction

Activity-driven alterations of gene expression patterns that consequently induce structural and functional changes in neurons are critical for long-term adaptations of brain circuits and indispensable for proper brain function, including learning and memory formation. Activity-elicited somatic calcium transients that drive nucleo-cytoplasmic shuttling of transcriptional regulators are believed to play a crucial role in this process (Greer & Greenberg, 2008; Hagenston & Bading, 2011). Moreover, a role of signaling through protein messengers, which translocate from the somatic cytoplasm or even from distal neuronal processes to the nucleus, has been reported recently (Jordan & Kreutz, 2009; Ch'ng & Martin, 2011). Though being not as fast as signaling through calcium waves, the translocation of messenger molecules provide more durable and specific signals and allow integration of temporarily or spatially segregated inputs. Despite their crucial role in neuronal plasticity, the molecular mechanisms that mediate activity-driven reconfiguration of gene expression are far from being completely understood.

C-terminal-binding protein 1/brefeldin A-ADP-ribosylation substrate (CtBP1/BARS), henceforth called CtBP1, is a multi-functional protein with well-established roles as a transcriptional co-repressor in the nucleus (Chinnadurai, 2007, 2009) and a regulator of membrane fission in the cytoplasm (Corda *et al*, 2006; Valente *et al*, 2013). It is a member of the CtBP protein family comprising also the ubiquitously expressed nuclear factor CtBP2 and the ribbon synapse-specific CtBP2 isoform RIBEYE (Katsanis & Fisher, 1998; Schmitz *et al*, 2000). In neurons, CtBP1 is highly enriched in the presynaptic compartment and, as in non-neuronal cells, in nuclei (tom Dieck *et al*, 2005; Jose *et al*, 2008; Hubler *et al*, 2012). In addition, a diffusely distributed cytoplasmic CtBP1 pool exists in all types of cells. Members of the CtBP family interact with the large presynaptic protein Bassoon (tom Dieck *et al*, 2005; Jose *et al*, 2008). Loss of this interaction was suggested to underlie the defects in ribbon anchoring to the presynaptic active zone in neurons lacking

1 Department of Neurochemistry and Molecular Biology, Leibniz Institute for Neurobiology, Magdeburg, Germany
2 Research Group Presynaptic Plasticity, Leibniz Institute for Neurobiology, Magdeburg, Germany
3 Center for Behavioral Brain Science, Otto von Guericke University, Magdeburg, Germany
4 Institute for Human Genetics, Otto von Guericke University, Magdeburg, Germany
5 Molecular Neurobiology, Medical Faculty, Otto von Guericke University, Magdeburg, Germany
*Corresponding author. Fax: +49 391 6263 92419; E-mail: gundelfi@lin-magdeburg.de
**Corresponding author. Fax: +49 391 6263 93319; E-mail: afejtova@lin-magdeburg.de
†Present address: Division of Neurophysiology, MRC National Institute for Medical Research, London, UK

functional Bassoon protein (Dick *et al*, 2003; tom Dieck *et al*, 2005; Khimich *et al*, 2005).

What is the function of presynaptic CtBP1? The reported role of CtBP1 in membrane trafficking is intriguing as neurotransmitter release relies on proper recycling of synaptic vesicles in presynaptic boutons (Alabi & Tsien, 2012). However, no structural or functional deficits were found at retinal ribbon synapses lacking functional CtBP1 (Vaithianathan *et al*, 2013). The dual synaptic and nuclear localization of CtBP1 suggests a function in communicating synaptic signals to the nucleus and hence in the activity-dependent regulation of neuronal gene expression. Little is known about the co-repressor function of CtBP1 in neurons. The repressor complex containing CtBP1 and neuronal-restrictive silencer factor (NRSF) has been implicated in the down-regulation of seizure-induced BDNF expression upon administration of anti-glycolytic compounds in the rat kindling model of temporal lobe epilepsy (Garriga-Canut *et al*, 2006). Another example is the CtBP1-mediated transcriptional repression of the gene encoding matrix-metalloproteinase 9, which is released upon neuronal depolarization (Rylski *et al*, 2008). However, it is currently unknown how CtBP1-mediated transcriptional repression is controlled by neuronal activity.

In this study, we tested the hypothesis that CtBP1 mediates synapto-nuclear signaling and contributes to the activity-induced reconfiguration of gene expression in neurons. We identified neuronal genes regulated by CtBP1 and demonstrated that activity-induced redistribution of CtBP1 between presynapses and nucleus underlies CtBP1-mediated transcriptional control of these genes. Moreover, our study revealed that CtBP1 is anchored to the presynapses via its direct interaction with the presynaptic cytomatrix proteins Bassoon and Piccolo. This association is regulated by cellular NAD/NADH levels (which in turn are activity regulated), restrains the size of the CtBP1 pool available for nuclear import, and thereby contributes to the control of activity-dependent gene expression.

Results

Neuronal activity controls the synapto-nuclear distribution of CtBP1 between presynapses and nucleus

Ultrastructural studies have established a localization of CtBP1 in presynapses of retinal photoreceptor and amacrine cells as well as in presynaptic boutons in the cerebellar molecular layer (tom Dieck *et al*, 2005; Hubler *et al*, 2012). In line with this, endogenous CtBP1 was detected in synapses and nuclei of cultured cortical neurons using immunostaining with antibodies against CtBP1 (tom Dieck *et al*, 2005; Supplementary Fig S1A). High-resolution dual-color stimulated emission depletion (STED) imaging revealed substantial overlap of CtBP1 immunoreactivity with the presynaptic marker Bassoon, while the postsynaptic marker Homer1 was aligned but clearly separated, similarly as it was found for co-staining of Bassoon and Homer. This confirms the presynaptic localization of CtBP1 in cultured neurons (Fig 1A).

To understand neuron-specific functions of CtBP1, we examined the activity-dependent distribution of endogenous CtBP1 at synapses and in nuclei of cultured cortical neurons. Chronic network activity silencing was induced by application of glutamate receptor antagonists 2-amino-5-phosphonovaleric acid (APV, 50 μM) and 6-cyano-7-nitroquinoxaline-2,3-dione (CNQX, 10 μM) for 48 h, a treatment which induces homeostatic presynaptic strengthening (Lazarevic *et al*, 2011). To increase the network activity, we treated cells with 4-aminopyridine (4AP, 2.5 mM) in combination with the GABAergic antagonist bicuculline (bicu, 50 μM) for 8 h. This treatment induces expression of activity-regulated genes (Xiang *et al*, 2007; Vashishta *et al*, 2009), including *BDNF*, which is regulated by the co-repressor function of CtBP1 (Garriga-Canut *et al*, 2006). CtBP1 immunofluorescence (IF) was significantly higher at individual synapses of highly active neurons compared with silenced cultures (Fig 1B and E; 115 ± 8% versus 69 ± 4% normalized to non-treated cells), whereas nuclear CtBP1

Figure 1. Neuronal activity regulates synapto-nuclear distribution of CtBP1.

A Dual-color stimulated emission depletion (STED) images of cultured hippocampal neurons, stained for CtBP1, Bassoon and Homer showing exclusive localization of CtBP1 at presynaptic sites.

B Representative images of primary cortical neurons (DIV 21) in cultures with basal activity levels or with elevated (4AP bicu) or blocked activity (APV CNQX) were stained with specific antibodies against CtBP1 and counterstained with synaptophysin 1 antibody to visualize synapses. Overlays are shown in colors as indicated.

C Representative images of neuronal cell bodies in cortical cultures with basal (control), elevated (4AP bicu), or blocked (APV CNQX) activity and with and without treatment with LB. Neurons were stained with antibody against CtBP1 and counterstained with DAPI to visualize cell nuclei.

D Total expression levels of CtBP1 in cell lysates from neurons with basal (control), blocked (APV CNQX), or enhanced activity are similar. GAPDH were used as a loading control. Bars and number on the left show position and size of Mw markers.

E, F Quantification of CtBP1 IF in synapses (E) and nuclei (F) in experiments shown in (B) and (C), respectively. Values are normalized to respective IF in cells with basal activity levels (dashed line on each graph).

G, H Block of protein synthesis (aniso, 6 h) or degradation (MG132 or lacta, 6 h) does not interfere with the activity-induced alterations of synaptic (G) or nuclear (H) CtBP1. Drugs were applied in cultures with basal, enhanced (4AP bicu, 6 h), or blocked (APV CNQX, 24 h) activity.

I Representative images of neuronal cell bodies in cortical cultures with basal (control) or elevated (4AP bicu) activity with and without treatment with LB. Neurons were stained with antibody against CtBP1 and counterstained with DAPI to visualize cell nuclei.

J Quantification of CtBP1 IF in nuclei in experiments shown in (I). Values are normalized to respective IF in cells with basal activity levels (dashed line on each graph).

Data information: The bar graphs (means ± SEM) display pooled data from two (J) or three independent neuronal cultures (E–H), for each bar *n* is indicated and stands for number of cells for measurement of nuclear CtBP1 IF or for visual fields containing ≥ 200 synapses for analysis of synaptic CtBP1 IF. Statistics was done by one-way ANOVA with Bonferroni *post hoc* test: ns, $P > 0.05$; ***$P < 0.001$. Indicated are comparisons with the control (indicated above each bar) and between conditions as horizontal bars. Scale bars are 0.3 μm (A, close-up), 1 μm (A, overview), 5 μm (B), and 10 μm (C, I).
Source data are available online for this figure

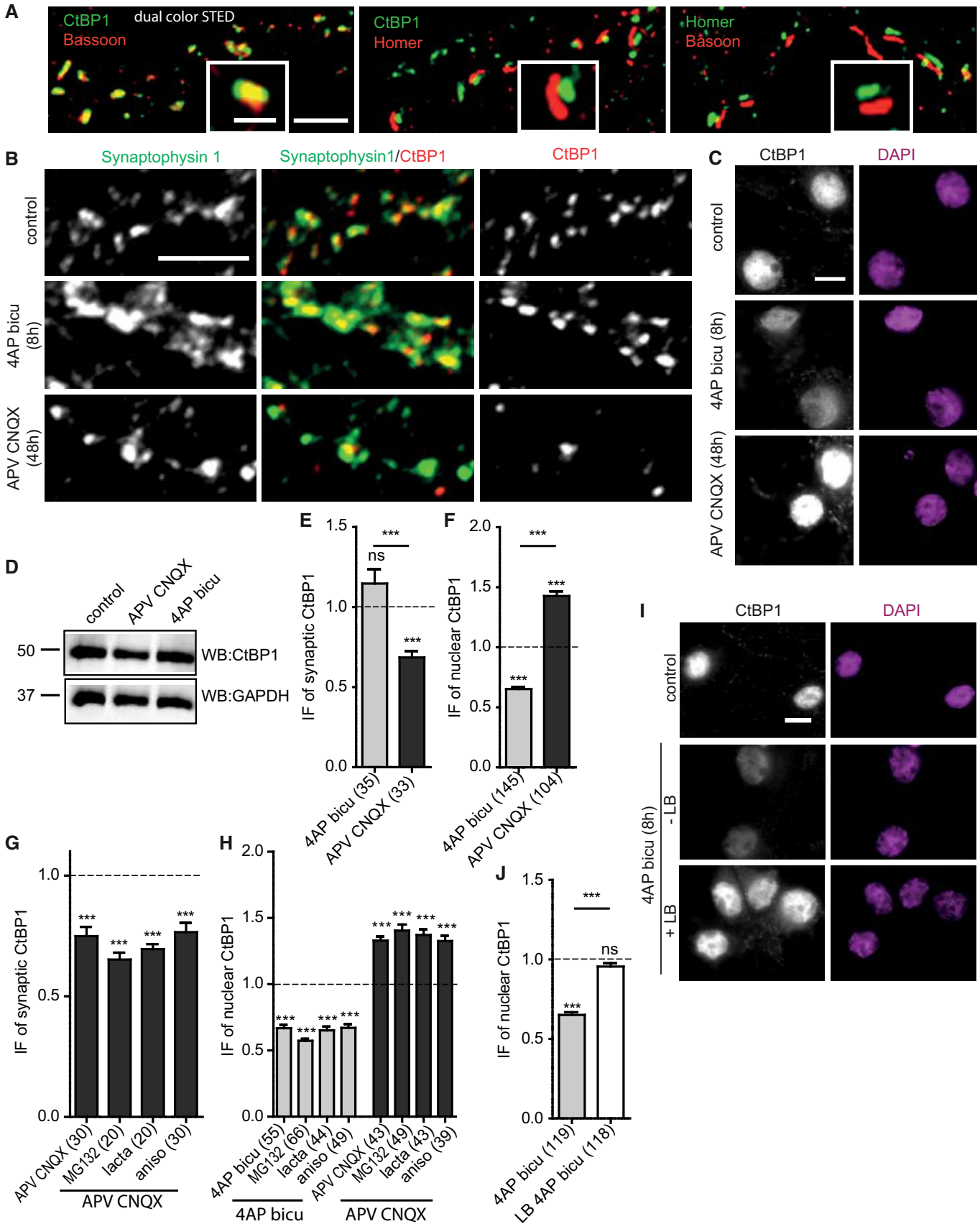

Figure 1.

dropped in overactive and raised in silenced cells (Fig 1C and F; 65 ± 1.8% versus 143 ± 3.8%). We observed a significant decrease of nuclear CtBP1 already 2 h after enhancement of the network activity (Supplementary Fig S1B and E). Block of glutamate receptors had to be applied for 24 h; 8-h-long treatment did not show any significant effect (Supplementary Fig S1C and F). Total expression levels of CtBP1 were not changed by activity modulation (Fig 1D; control: 100 ± 2.4%, APV CNQX: 95 ± 8%, 4AP, bicu 116 ± 10%; normalized to control). Block of protein synthesis with anisomycin (aniso, 10 μM, 6 h) or inhibition of proteasome-mediated degradation with MG132 (10 μM, 6 h) or with lactacystin (lacta, 0.5 μM, 6 h) did not affect the activity-induced shift in synapto-nuclear distribution of CtBP1. These results imply that activity modulation induces a redistribution of CtBP1 between its synaptic and nuclear pool rather than independent regulation of CtBP1 turnover in specific compartments [Fig 1G and H; nuclei (normalized to control): 4AP bicu MG132: 57 ± 1.6%, 4AP bicu lacta: 65 ± 1.6%, 4AP bicu aniso: 67 ± 2.7%, APV CNQX MG132: 141 ± 4.5%, APV CNQX lacta: 137 ± 4.3%, APV CNQX aniso: 133 ± 4%; synapses: APV CNQX MG132: 65 ± 2.8%, APV CNQX lacta: 70 ± 2.1%, APV CNQX aniso: 77 ± 3.8%]. Moreover, a block of nuclear export using leptomycin B (LB; 3 nM, 8 h) completely prevented the decline of nuclear CtBP1 in the condition of enhanced neuronal activity (Fig 1I and J; control: 100 ± 2.3%; 4AP, bicu: 65 ± 1.9%; 4AP, bicu, LB: 96 ± 2.3%), indicating an activity-induced physical translocation of CtBP1 from nucleus to cytoplasm.

CtBP1 undergoes retrograde and anterograde translocation between synapses and cell bodies in neurons

To test the possibility of physical translocation of CtBP1 between synapses and cell bodies, we performed live imaging experiments using internally tagged CtBP1 construct containing EGFP (CtBP1intEGFP) or photoactivatable EGFP (CtBP1intPAEGFP) (Patterson & Lippincott-Schwartz, 2002) (Fig 2A). CtBP1intEGFP, expressed using lentiviral vectors, showed a distribution and abundance similar to the endogenous CtBP1 in COS-7 cells (not shown) and in cultured hippocampal neurons, where it was localized to nucleus and presynapses (Fig 2B and C). The presynaptic targeting of the expressed CtBP1intEGFP was evident by its presence in synapses formed on dendrites of non-transduced cells (Fig 2B), while spines of infected neurons were not labeled (Fig 2C). The presynaptic localization of CtBP1 was further confirmed using high-resolution dual-color STED showing a neat alignment with Bassoon and lack of co-localization with the postsynaptic marker Homer (Fig 2D).

Spatially restricted photoactivation (PA) allowed us to separately follow the fate of CtBP1intPAEGFP photoactivated in the somatic/nuclear compartment or in the active presynapses (Fig 3A and C, respectively). A decay of the CtBP1intPAEGFP fluorescence (F^{PAEGFP}) initially photoactivated in a circular somatic region containing the cell nucleus and a concomitant increase of the F^{PAEGFP} in active synapses identified by synaptotagmin 1 antibody (Syt1 Ab) uptake (Kraszewski *et al*, 1995) were evident 2 h after PA (Fig 3A and B). To assess its retrograde flow, we specifically photoactivated CtBP1intPAEGFP in active synapses marked beforehand by Syt1Ab uptake. We observed a decline of F^{PAEGFP} in the photoactivated synapses, while a significant augmentation of F^{PAEGFP} was detected in the adjacent cell bodies 3 h after PA (Fig 3C and D). This rise of F^{PAEGFP} was not due to increasing autofluorescence or spontaneous photoconversion of PAEGFP during prolonged imaging as shown by imaging of cells in a parallel experiment without PA (Supplementary Fig S2). The anterograde translocation of CtBP1 is compatible with the common view of trafficking of newly synthesized proteins from cell bodies to their synaptic destination. However, the retrograde translocation of CtBP1 is unexpected and in line with its potential function as a retrograde molecular messenger.

Neuronal activity controls synaptic retention of CtBP1

To test whether regulation of the synaptic retention is implicated in the redistribution of CtBP1 between synapses and soma/nucleus upon activity modulation, we assessed the dynamics of the synaptic CtBP1intPAEGFP in highly active and in silenced neurons. We blocked or elevated the neuronal network activity by application of the sodium channel blocker tetrodotoxin (TTX, 2 μM) or the potassium channel blocker 4AP (100 μM) (Mihaly *et al*, 1983; Voskuyl & Albus, 1985), respectively, immediately before the PA experiments and quantified F^{PAEGFP} loss in the photoactivated synaptic regions specified beforehand by Syt1 Ab uptake (Fig 4A). Acute and chronic block of neuronal activity enhanced the F^{PAEGFP} loss (Fig 4B; TTX: 57 ± 1.1%, APV CNQX: 51 ± 1.5% of initial F^{PAEGFP}), as compared to cultures with basal activity levels (control: 76 ± 1.6%), whereas an increase of the neuronal activity attenuated the F^{PAEGFP} loss (4AP: 89 ± 1.3%) 3 h after PA.

Photoactivation may lead to overestimation of the synaptic exchange rates due to a spontaneous loss of F^{PAEGFP} or degradation of the photoactivated PAEGFP. Therefore, we also applied fluorescence recovery after photobleaching (FRAP) as an alternative method and tested very acute effects of activity modulation. CtBP1intEGFP-expressing synapses were bleached, and FRAP was monitored for the following 325 s (Fig 4C). In cultures with basal activity levels, CtBP1intEGFP fluorescence (F^{EGFP}) recovered to around 60% after 300 s, indicating substantial synaptic dynamics of CtBP1 (Fig 4C–E). We found a significant FRAP reduction after treatment with 4AP (100 μM) for 20–40 min before bleaching (Fig 4C, D and F; 14.5 ± 2.9% less than control). On the contrary, chronic silencing for 48 h before the experiment accelerated the FRAP rates (Fig 4C, E and F; 14.1 ± 2.3% increase relative to control). Taken together, the live imaging experiments strongly suggest that neuronal activity regulates the molecular dynamics of synaptic CtBP1. Inactivity significantly accelerates CtBP1 dissociation from the synaptic structures, whereas elevated network activity leads to an increase in the synaptic retention of CtBP1.

Nucleo-cytoplasmic shuttling of CtBP1 underlies activity-driven transcriptional regulation in neurons

Studies performed in non-neuronal cells have shown that the co-repressor activity of CtBP1 is controlled by regulation of its nuclear localization (Barnes *et al*, 2003; Verger *et al*, 2006). Therefore, we asked whether the activity-dependent changes in the abundance of nuclear CtBP1 were causally linked to the expression of neuronal

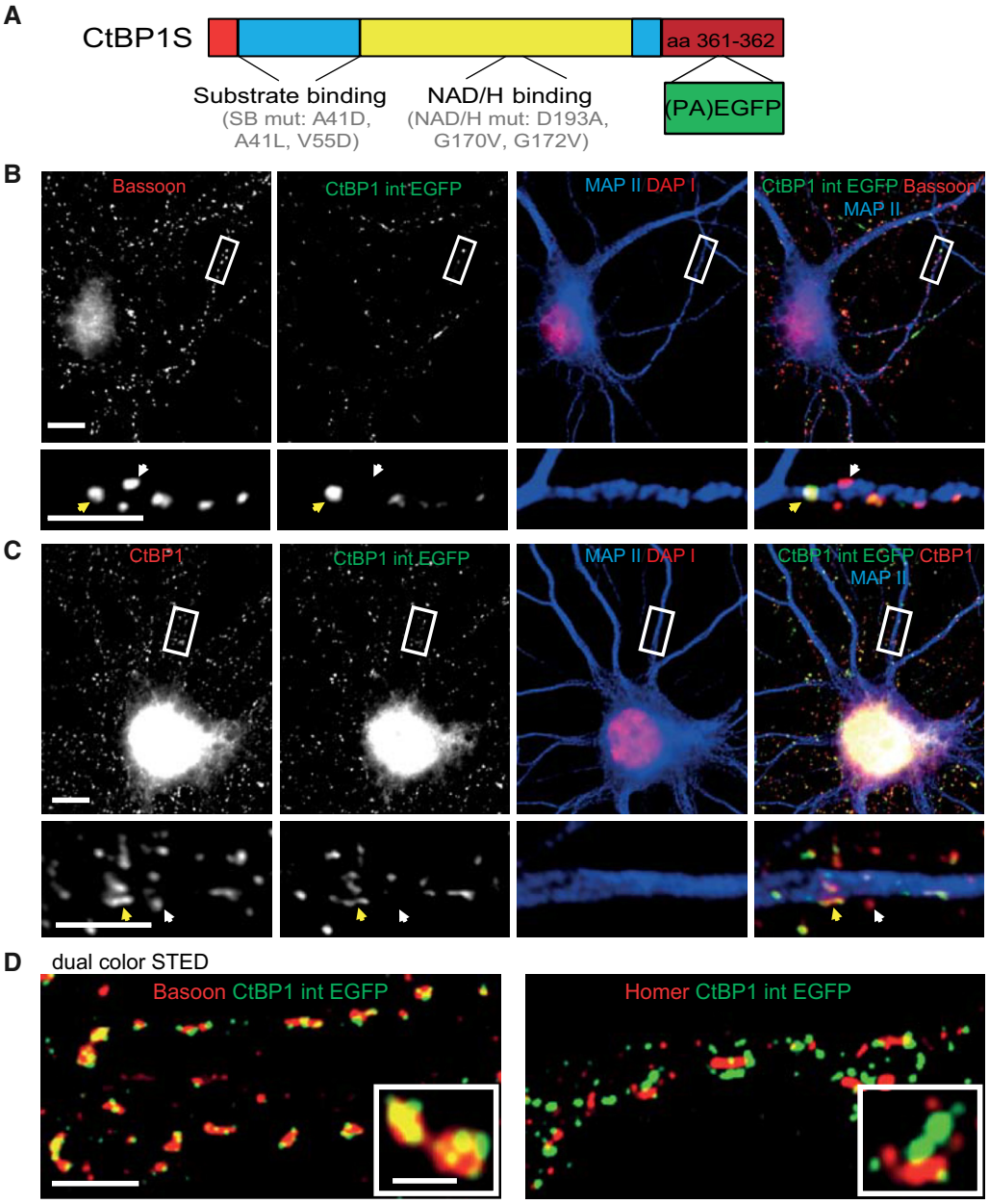

Figure 2. Expressed CtBP1intEGFP displays correct targeting to presynaptic sites and to nucleus.

A Scheme showing the domain structure of CtBP1; positions of mutations used in this study and insertion of (PA)EGFP between amino acids 361 and 362 are indicated.

B, C CtBP1intEGFP expressed in primary hippocampal neurons is localized correctly to presynaptic terminals and to nucleus. CtBP1intEGFP containing synapses (marked by presynaptic marker Bassoon) formed by axons of a transduced neuron on dendrites of a non-transduced neuron (yellow arrow) is shown in (B). White arrows depict Bassoon-positive presynaptic terminals not containing CtBP1intEGFP, likely formed by non-transduced axons. CtBP1intEGFP localized correctly in the nucleus and in autapses that neuron forms on itself is shown in (C). Correspondingly, only some synapses on the dendrites of the transduced neuron contain CtBP1intEGFP (yellow arrows) despite the ubiquitous synaptic expression of endogenous CtBP1 (white arrows). Nuclear staining of CtBP1 and CtBP1intEGFP is saturated in order to show synaptic CtBP1, for lower intensity nuclear staining see Fig 5D.

D Dual-color stimulated emission depletion (STED) images demonstrate tight co-localization of CtBP1intEGFP with the presynaptic marker Bassoon and apposition with the postsynaptic marker Homer, confirming its targeting to presynapses.

Data information: Overlays are shown in colors as indicated. Scale bars are 10 μm on the overview and 5 μm on the close-up images (B, C), 1 μm (D, overview), and 0.3 μm (D, close-up).

activity-regulated genes. CtBP1 directly interacts and controls the transcriptional activity of NRSF, which in turn regulates *BDNF* transcription from promoter I+II, containing the NRSF binding site RE1 (Garriga-Canut *et al*, 2006; Hara *et al*, 2009). Therefore, we examined whether BDNF promoter I+II activity co-varies with the nuclear abundance of endogenous CtBP1. To this end, we used a reporter of

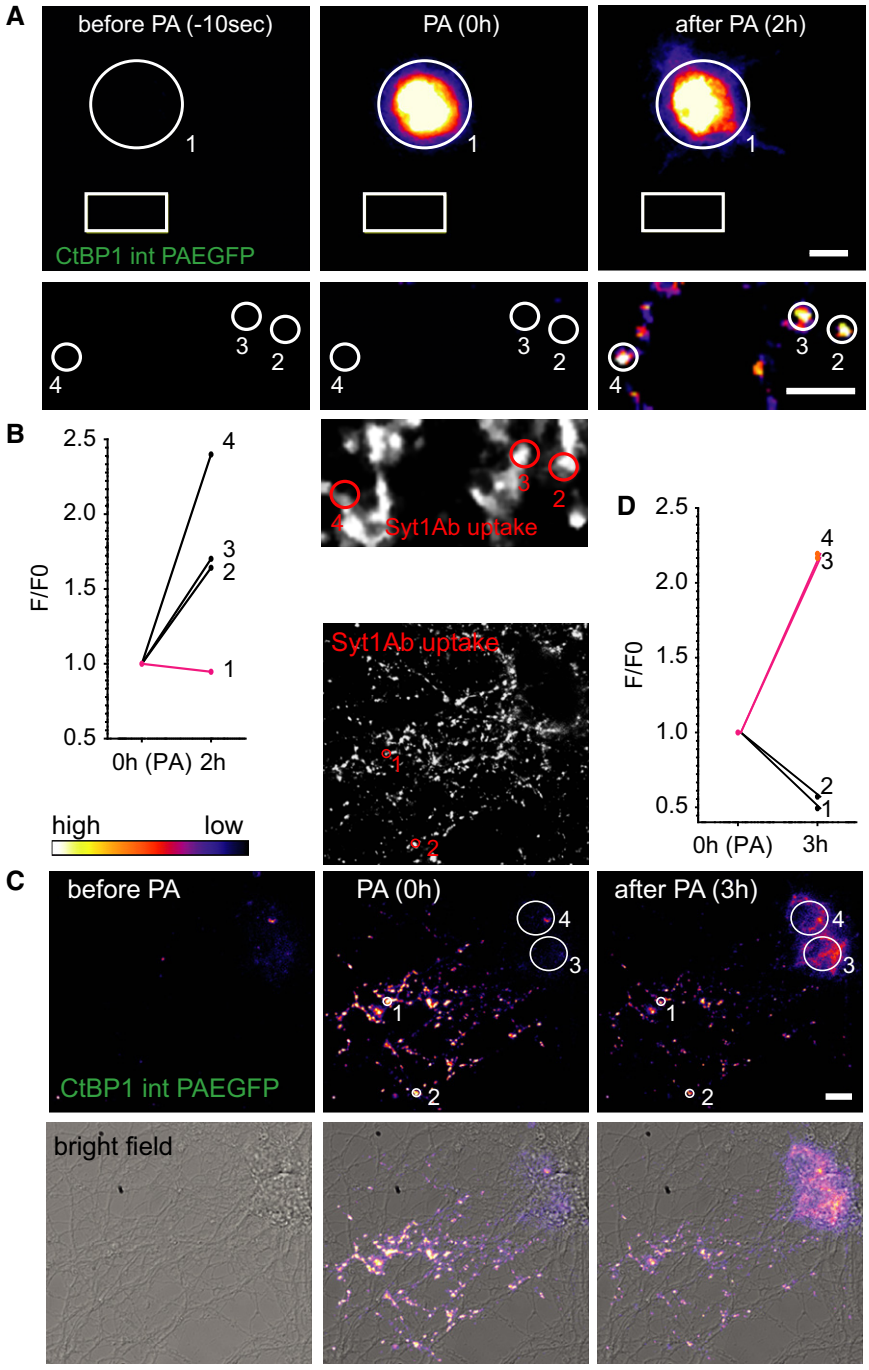

Figure 3. CtBP1 translocates between presynapses and soma/nuclei.

A, B CtBP1intPAEGFP photoactivated in the nucleus translocates to synapses 2 h after PA. Active presynaptic terminals were labeled using Syt1 Ab uptake. In order to show synaptic F^{PAEGFP} close-up images are shown with higher gain than the overview image. F^{PAEGFP} changes in the respective regions depicted in (A) are shown in (B).

C, D CtBP1intPAEGFP photoactivated at synapses labeled using Syt1 Ab uptake beforehand can be detected in nucleus/soma 3 h after PA. The synaptic F^{PAEGFP} declines accordingly. F^{PAEGFP} changes in the respective regions depicted in (C) are shown in (D).

Data information: Scale bars are 10 μm on the overview image (A, C) and 5 μm on the close-up in (A).

BDNF promoter I+II activity (BDNFpI+IIEGFP), where EGFP was expressed under the control of the 5′-part of the *BDNF* gene (Supplementary Fig S3A) (Hara *et al*, 2009). A quantitative analysis revealed significant negative correlation between the nuclear IF intensities of endogenous CtBP1 and the BDNFpI+II-driven expression of EGFP at a level of individual cells (Supplementary Fig S3A; Pearson $r = -0.47$, $P = 0.0113$). Consistently, activity enhancement leading to a depletion of nuclear CtBP1 induced expression of

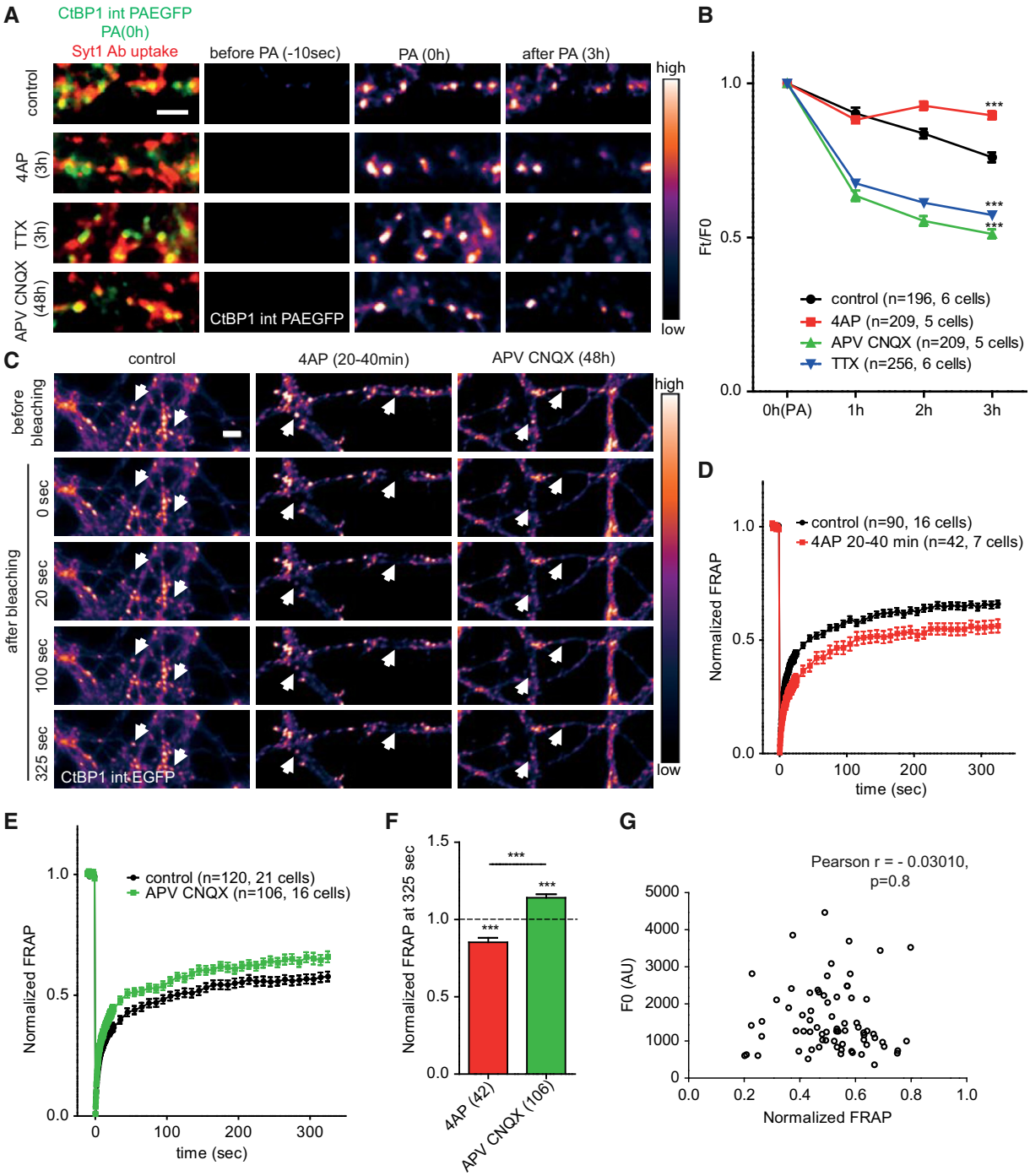

Figure 4. Neuronal activity regulates synaptic retention of CtBP1.

A PA of synaptic CtBP1intPAEGFP in hippocampal neurons with basal activity (control) and upon activity modulation as indicated. Active presynaptic terminals were labeled by Syt1 Ab uptake before PA.

B Quantification of the experiment shown in (A). Average F^{PAEGFP} at 1, 2, and 3 h (Ft) after PA are shown normalized to the F^{PAEGFP} at time of PA (F0). Statistics were done on data from 3 h post-PA.

C–G Fluorescence recovery after photobleaching (FRAP) experiments on synaptic CtBP1intEGFP in neurons with control, enhanced, or low network activity. Representative images are shown in (C); arrows point to bleached areas. Averaged FRAP traces for cultures with increased (D) or silenced (E) synaptic activity always compared to parallel cultures with basal activity. Quantification of recovery (F) at 325 s after bleaching in experiments shown in (C); values are normalized to recovery in cultures with basal activity (dashed line in graph). Lack of correlation between initial F^{EGFP} and normalized FRAP at 325 s at individual synapses (G) suggests that differences in basal activity level rather than expression levels of CtBP1intEGFP explain observed variability of FRAP rate between experiments.

Data information: The graphs display means ± SEM of pooled data from ≥ 2 neuronal cultures; number of synapses (*n*) and number of independent cells are indicated. Statistics were done as in Fig 1. Scale bars are 5 μm. ***$P < 0.001$.

Figure 5. CtBP1 controls expression of activity-regulated genes in neurons.

A Transcripts of 14 activity-regulated genes are regulated in cultured cortical neurons expressing CtBP1KD944. Statistical significance in comparison with expression of scrambled is given above each bar.

B, C CtBP1intEGFP rescues the effect of CtBP1KD944 on the expression of Arc (B) and BDNF (C) mRNA levels, while EGFP-CtBP1 fails to do so.

D Representative images showing the synapto-nuclear distribution of endogenous CtBP1 and expressed CtBP1intEGFP and EGFP-CtBP1 in cultured hippocampal neurons. Neurons were stained for Bassoon to label presynapses; DAPI labels nuclei. Note that EGFP-CtBP1 displays an aberrant nuclear localization.

E, F Activity-induced gene expression in control and CtBP1KD944 neurons (E) and upon nuclear export block by LB in CtBP1KD944 and control neurons (F). Values are normalized to expression in neurons with basal activity levels (E, dashed line) and to activity-induced expression in untreated cells (F, dashed line).

Data information: The graphs display means ± SEM. Numbers of independent cultures (A) or qPCRs on independent cDNA preparations from 2 (E, F) or ≥ 3 cultures (B, C) are given in brackets. Statistical significance was assessed by Student's *t*-test in (A), (E), and (F) and one-way ANOVA with Dunett *post hoc* test (B, C): ns, $P > 0.05$; *$P < 0.05$; **$P < 0.01$; ***$P < 0.001$. Scale bar is 10 μm (D).

BDNFpI + IIEGFP reporter (Supplementary Fig S3C and E; 287 ± 39% of control), while activity silencing resulted in a nuclear accumulation of CtBP1 and a down-regulation of the reporter (Supplementary Fig S3D and F; 60 ± 8.4%).

To assess whether CtBP1 is implicated in the regulation of activity-dependent gene transcription, we analyzed the effect of CtBP1 depletion on the expression of 84 selected activity-regulated genes using quantitative real-time PCR (qPCR) array. We interfered with the expression of CtBP1 by lentivirus-driven expression of two independent short hairpin RNAs (shRNAs): 467 and 944. Their knockdown efficiency and specificity were confirmed by quantitative Western blots of cell lysates from infected cultures (Supplementary Fig S3G and H). From 84 genes tested, the expression of 14 was consistently changed in neurons upon CtBP1 knockdown with shRNAs 944 or 467 (CtBP1KD944 or 467) as compared to scrambled controls (Fig 5A and Supplementary Fig S3I). Depletion of CtBP1 caused in most cases an up-regulation of the target genes (i.e. *Arc, Bdnf, Egr1, Egr4, Fos, Junb, Ntf3, Ntf4, Ngfr, Gabra5, Grin2a, Grm2*), which is in line with the described co-repressor function of CtBP1 (Chinnadurai, 2007). However, we also observed a significant down-regulation of *Camk2a* and *Prkg1* (Fig 5A and Supplementary Fig S3I). Expression of a CtBP1intEGFP construct, resistant to the shRNA 944, in CtBP1KD944 cultures fully compensated the shRNA-induced release of BDNF and Arc repression, further confirming both the specificity of the shRNA approach and the functionality of CtBP1intEGFP construct (Fig 5B–D).

Interestingly, seven out of the 14 genes regulated in neurons upon CtBP1 knockdown showed analogous regulation upon pharmacological enhancement of neuronal activity for 8 h (Fig 5E, Supplementary Table S1), which also leads to a prominent lowering of CtBP1 nuclear levels (see Fig 1). Thus, we next asked whether CtBP1 is required for the activity-driven regulation of these seven gene targets. To address this, we assessed the activity-induced gene expression in control and CtBP1KD944 cultures treated with 4AP and bicu. CtBP1KD944 significantly interfered with the activity-dependent regulation of the selected genes (Fig 5E, Supplementary Table S1), indicating an important role of CtBP1 in the transcriptional regulation of the tested activity-driven genes. To assess the importance of the nucleo-cytoplasmic translocation of CtBP1 in the activity-dependent gene transcription we blocked the active nuclear export with LB (see Fig 1I and J). LB treatment largely suppressed activity-induced transcriptional regulation in control neurons, but had significantly milder effects in CtBP1KD944 neurons (Fig 5F, Supplementary Table S1). Thus, the observed LB effects depend on CtBP1 expression, most likely due to interference with the nuclear export of CtBP1. In line with this, overexpressed EGFP-CtBP1 construct, which localizes to synapses but not to nucleus, was not able to rescue the elevated expression of Arc and BDNF in CtBP1KD944 cultures (Fig 5B–D).

Bassoon and Piccolo regulate the synaptic versus nuclear distribution and the co-repressor activity of CtBP1

To understand the mechanism underlying the activity-dependent regulation of synaptic CtBP1 (Figs 1 and 3), we studied how CtBP1 is anchored to the presynaptic structures. Bassoon, a presynaptic scaffold protein interacting with CtBP1 (tom Dieck *et al*, 2005; Jose *et al*, 2008), seems not to be the exclusive presynaptic anchor for CtBP1 as in neurons from Bassoon-mutant mice ($Bsn^{-/-}$) (Hallermann *et al*, 2010), the synaptic CtBP1 is reduced (63 ± 1.5% of WT) but not completely abolished (Supplementary Fig S4A and D). Thus, we tested a potential binding to Piccolo, a paralogue of Bassoon sharing significant structural homology and functional redundancy (Fenster *et al*, 2000). We identified amino acid sequences resembling the prototypical PXDLS motif, described to mediate the interaction with the substrate-binding domain (SBD) of CtBPs, in both the fragment of Bassoon RB46 (aa 1,653–2,087) reported to bind to CtBPs (tom Dieck *et al*, 2005), and in the fragment RP16 covering a homologous region (aa 2,668–2,985) of rat Piccolo (Fig 6A). We confirmed an interaction between PXDLS motif-containing Piccolo fragments and CtBP1 in a yeast two-hybrid (Y2H) system (Fig 6A) and in pull-down experiments using bacterially expressed fusion constructs (Fig 6B). We detected CtBP1 in the subcellular fraction containing the specialized Piccolo–Bassoon transport vesicles (PTVs) immuno-isolated from juvenile brain tissue, suggesting that CtBP1 associates with membrane-associated Bassoon and Piccolo during their transport toward the nascent synapses (Fig 6C). Moreover, synaptic CtBP1 was reduced upon RNA interference-driven depletion of Piccolo with shRNA Pclo28 (Leal-Ortiz *et al*, 2008) to a similar extent as in $Bsn^{-/-}$ neurons (Supplementary Fig S4B and E; Pclo28: 81 ± 1.8% of WT scrambled). To ultimately test whether the synaptic localization of CtBP1 is dependent on Bassoon and Piccolo, we tested CtBP1 localization in cultured hippocampal neurons from mouse mutants for both Bassoon and Piccolo (DKO). Strikingly, CtBP1 staining was completely lost at the synapses of DKO neurons, whereas the staining in the nucleus was still present (Fig 6D) and the total expression levels of CtBP1 were not affected (Supplementary Fig S4F and G). In line with that, synaptic CtBP1 was also strongly reduced upon shRNA Pclo28-induced depletion of Piccolo in $Bsn^{-/-}$ neurons (Supplementary

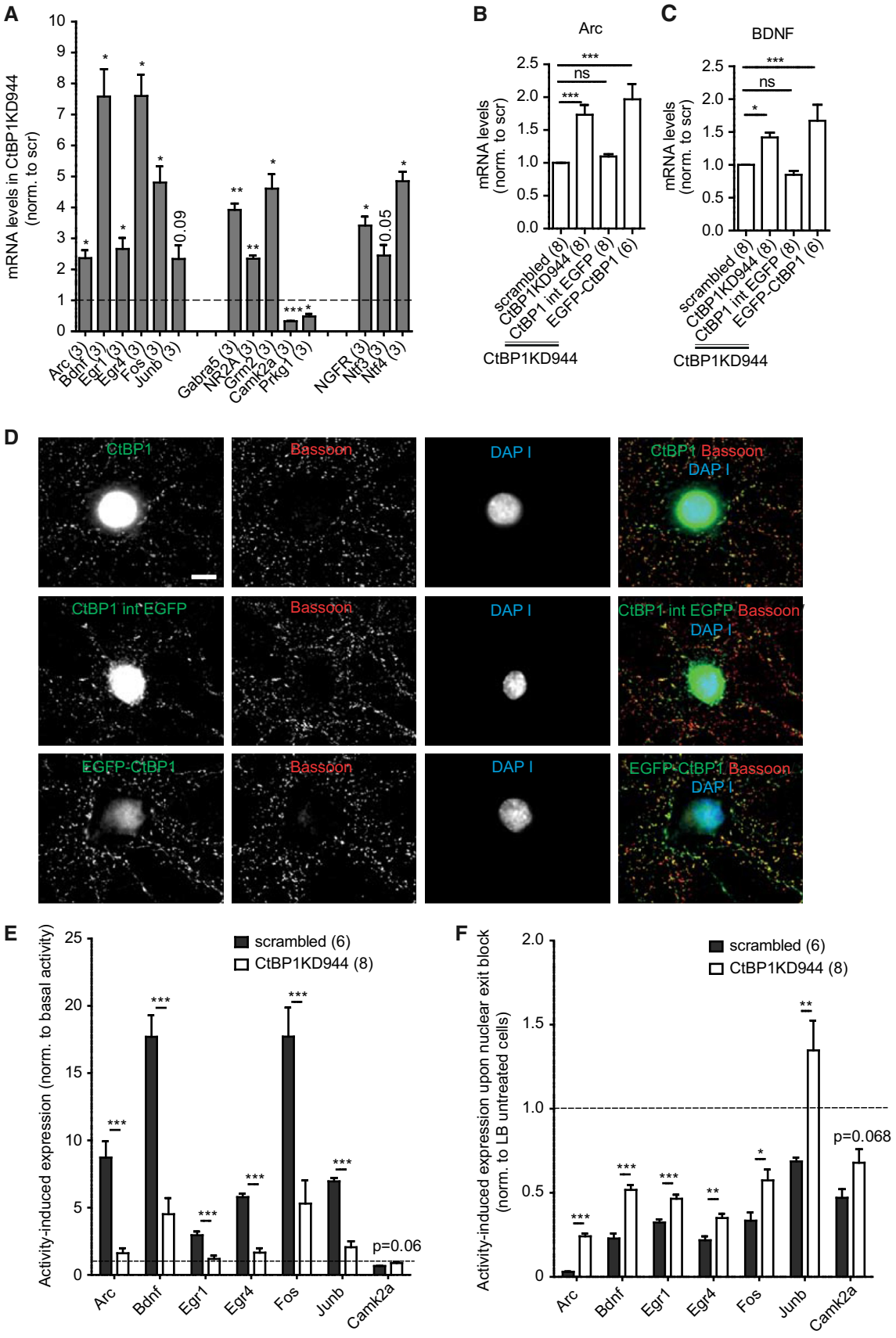

Figure 5.

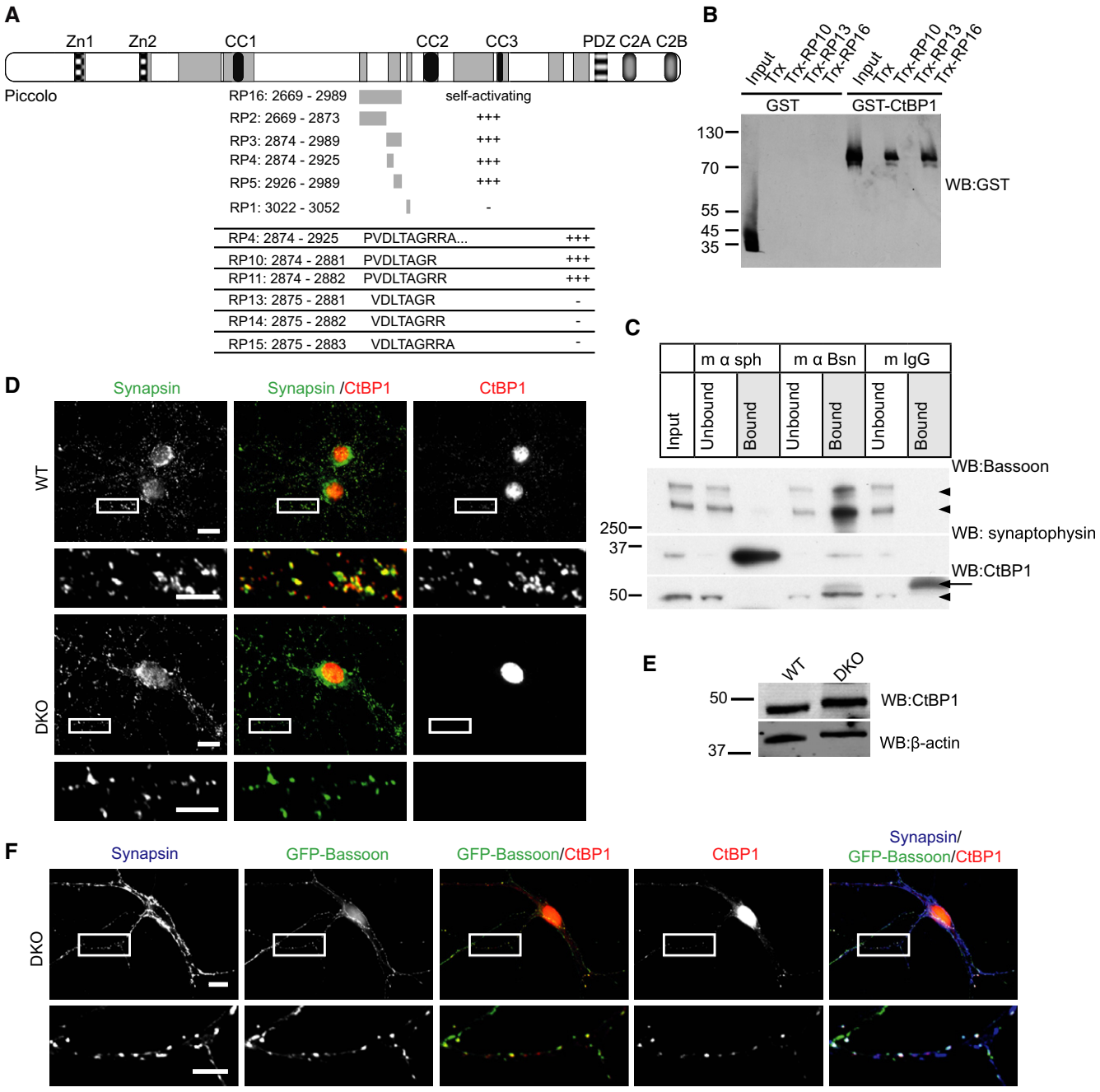

Figure 6. Bassoon and Piccolo control the synapto-nuclear distribution of CtBP1.

A Domain structure of rat Piccolo with structural domains: Zn1,2, zinc fingers; CC, coiled coil regions; PDZ, PSD-95/Dlg/zonula occludens-1 homology domain; and C2, PKC conserved region 2; gray boxes show the regions of high Bassoon–Piccolo homology. The position or aa sequence of fragments used for Y2H and biochemical interaction studies is depicted; the numbers show corresponding aa residues. In Y2H, none (–) or strong (+++) reporter gene activation was observed.

B Pull-down assays demonstrating a direct interaction of GST-CtBP1 with immobilized Trx-RP10 (covering a minimal binding motif of Piccolo) and RP16, but not with N-terminally shortened Trx-RP13. GST alone did not bind to any of the tested Piccolo fragments.

C CtBP1 co-purifies with PTVs, precipitated with Bassoon antibody (m α Bsn), and is absent from the synaptic vesicle precursors (SVPs) isolated with synaptophysin antibody (m α sph) or in control isolation using unspecific IgG. Arrowheads mark specific bands for Bassoon, synaptophysin, and CtBP1; additional bands detected with an anti CtBP1 antibody (arrow) correspond to the IgG heavy chain.

D CtBP1 localizes to synapses and nucleus in hippocampal neurons prepared from WT mice, but is present only in nucleus in neurons from DKO mice.

E Immunoblot shows that the total expression levels of CtBP1 in cultured neurons at DIV 14 are not different between genotypes. Detection of β-actin was used as a loading control.

F Expression of GFP-Bsn in DKO rescues the synaptic localization of CtBP1.

Data information: Bars and numbers in left show position and size of Mw markers in Western blot images. Scale bars are 10 μm for the overview and 5 μm for the close-ups (D, F).

Fig S4H and I). No changes in the presynaptic composition were reported in neurons from Piccolo mutants expressing shRNA against Bassoon (Mukherjee *et al*, 2010), supporting specificity of the synaptic loss of CtBP1. Expression of GFP-Bsn (Dresbach *et al*, 2003) in DKO neurons rescued the synaptic localization of CtBP1 in axons of transfected cells (Fig 6F), further confirming that CtBP1 localizes to synapses via its interaction with Bassoon (and Piccolo) and that at least one of the two proteins is necessary and sufficient for the synaptic localization of CtBP1.

Depletion of the synaptic pool of CtBP1 affects activity-dependent nucleo-cytoplasmic shuttling of CtBP1

Neurons from DKO animals, where the synaptic pool of CtBP1 is essentially depleted, offer an opportunity to investigate whether the synaptic and the nuclear pool of CtBP1 functionally influence each other. A quantitative IF analysis of endogenous CtBP1 revealed its substantial nuclear accumulation in neurons from DKO animals compared to their wild-type (WT) siblings (126 ± 5% of WT neurons; Fig 7A and B). Total expression levels of CtBP1 were not significantly altered as shown by quantitative Western blot of brain homogenates from newborn mice (Supplementary Fig S4F and G; WT: 100 ± 7.8%; $Bsn^{-/-}$: 84 ± 5.9%; Pclo3: 102 ± 4.6%; DKO: 99 ± 4.5%) or of lysates from cultured hippocampal neurons grown for 14 DIV (Fig 6E, WT: 100 ± 23%, DKO: 87 ± 10%). Thus, loss of its synaptic anchors lead to a redistribution of CtBP1 finally resulting in its higher nuclear abundance. Consistently, the expression of BDNFpI+IIEGFP reporter was significantly reduced in DKO neurons (59 ± 5% of WT neurons) in comparison with WT (Fig 7A and C). To test whether the loss of synaptic CtBP1 affects activity-induced regulation of the nuclear levels of CtBP1, we modulated the network activity in cultured hippocampal neurons from DKO mice and their WT siblings and quantified the changes in the nuclear CtBP1. As expected in WT, the treatments induced significant alterations in the nuclear CtBP1 (Fig 7D and E; 4AP, bicu: 78 ± 2.9% of control; APV CNQX: 118 ± 5.8%) similar to what we observed in rat cortical neurons (Fig 1C and F). The DKO neurons responded to the treatments by changes in the release as shown by Syt1 Ab uptake (Supplementary Fig S5), but neither activity enhancement (Fig 7D and F; 94 ± 4.9%) nor silencing (Fig 7D and F; 87 ± 4.2%) had any significant effect on the nuclear CtBP1 in these neurons. Thus, normal synaptic anchoring of CtBP1 importantly contributes to activity-dependent regulation of the nuclear levels of CtBP1.

Bassoon and Piccolo interact via their PXDLS motifs with the SBD of CtBP1. In line with this, mutations A41D, A41L, or V55D inactivating the substrate-binding pocket of CtBP1 (Fig 2A) (Nardini *et al*, 2003) interfered with its binding to RB46 in Y2H assay. The SBD also mediates the interaction of CtBP1 with most of its nuclear binding partners, which is required for its nuclear import and function as a transcriptional co-repressor (Nardini *et al*, 2003; Kuppuswamy *et al*, 2008). This implies that Bassoon and Piccolo might compete with CtBP1-binding nuclear factors for the same binding site, sequester CtBP1 and make it unavailable for nuclear import and co-repression. To test this hypothesis, we over-expressed GFP-Bsn in COS-7 cells, which normally do not express Bassoon, and examined the sub-cellular distribution of the endogenous CtBP1. GFP-Bsn formed characteristic ectopic clusters in the cytosol of the transfected cells, which sequestered endogenous CtBP1 (Fig 7G). Consequently, the IF of CtBP1 was significantly reduced in the nuclei of cells expressing GFP-Bsn compared with cells expressing EGFP alone (Fig 7G and H; GFP-Bsn transfected cells: 77 ± 5%, EGFP transfected cells: 110 ± 5.8%; normalized to untransfected cells), suggesting that Bassoon can sequester CtBP1 and thereby regulates its nuclear localization.

Neuronal NAD/NADH ratio controls the molecular dynamics of CtBP1 at synapses and its subcellular localization via modulation of its affinity to Bassoon

Next, we tested whether activity regulates the synaptic retention of CtBP1 via modulation of the binding to its synaptic anchor Bassoon. As regulation of the synaptic association of CtBP1 should precede its synapto-nuclear redistribution, we tested acute effects of activity modulation. Activity enhancement for 30 min led to a significant increase in the co-immunoprecipitation (co-IP) of Bassoon with CtBP1intEGFP overexpressed in primary cortical cultures (Fig 8A and B; 4AP bicu: 125 ± 5.3% of co-IP in basal activity), indicating modulation of CtBP1-Bassoon interaction by neuronal activity.

CtBPs bind to nicotinamide adenine dinucleotides NAD and NADH, which critically influences the affinity of CtBP1 for its PXDLS motif-containing binding partners (Zhang *et al*, 2002). To test whether NAD or NADH modulates association of CtBP1 with Bassoon, we performed a quantitative co-IP of CtBP1intEGFP and Bassoon fragment RB29 (aa 1,692–3,262; Dresbach *et al*, 2003) (Fig 8C) over-expressed in HEK293T cells in the presence of increasing concentrations of NAD or NADH. Rising (but still physiological) concentrations of NADH significantly stimulated the binding (Fig 8D and E; NADH 100 nM: 131 ± 5.5%, 10 μM: 141 ± 9.9% and 100 μM 147 ± 10% of control), while raising the NAD concentration had no effect on RB29-CtBP1 interaction (Fig 8D and E). Next, we treated HEK293T cells expressing RB29 and CtBP1intEGFP with 2-deoxy-D-glucose (2DG, 10 mM, 24 h)—a potent inhibitor of glycolysis, which depletes the cellular NADH. Co-IP of RB29 with CtBP1intEGFP was significantly lower in 2DG-treated cells (Fig 8F and G; 2DG co-IP: 66 ± 4.2% of control co-IP) confirming the positive modulatory role of NADH. A co-IP of RB29 with CtBP1 mutant containing D193A, G170V and G172V substitutions inactivating its NAD/NADH-binding site (see Fig 2A) (Kumar *et al*, 2002) was not affected by the 2DG treatment (Fig 8F and G) confirming that direct NAD/NADH binding to CtBP1 is essential for modulation of its interaction with Bassoon in cellular context. Interestingly, this mutant does not localize to synapses, if expressed in neurons (Supplementary Fig S6A), which is in line with a dependence of CtBP1 synaptic localization on its interaction with Bassoon and Piccolo.

If CtBP1 localizes to synapses via interaction with Bassoon and Piccolo which is enhanced by increasing NADH levels, then synaptic retention of CtBP1 should be affected upon manipulation of the NADH levels in neurons. To examine this, we measured FRAP of CtBP1intEGFP in neurons treated with 2DG (5 mM, 48 h). This treatment did not affect cell viability (Supplementary Fig S6G and H). The recovery was significantly higher upon 2DG treatment (Fig 9A and B, 116 ± 2.5% of the control), which is in line with a weaker association of CtBP1 with Bassoon at synapses under these conditions. We also found a decrease in the NAD/

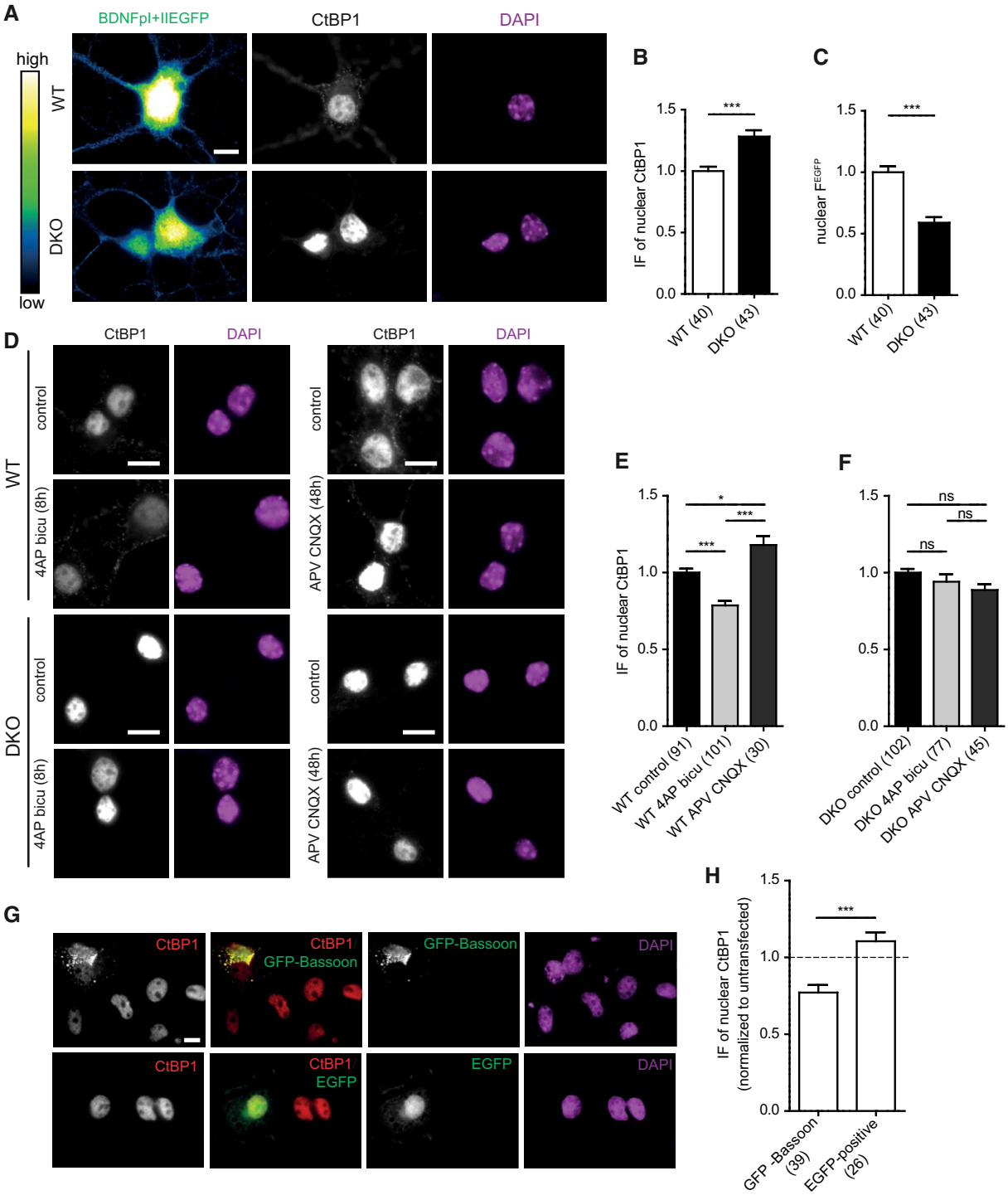

Figure 7. Activity-induced synapto-nuclear shuttling of CtBP1 is impaired in DKO neurons.

A Expression of BDNFpI+IIEGFP reporter in WT and DKO neurons counterstained for CtBP1 and with DAPI.

B, C Quantification of the nuclear IF of CtBP1 (B) and nuclear F^{EGFP} driven by BDNFpI+II (C) in hippocampal neurons from WT and DKO mice.

D Examples of shuttling of CtBP1 upon pharmacological modulation of neuronal activity levels in hippocampal neurons from WT and DKO animals.

E, F Quantification of nuclear CtBP1 IF in the experiment shown in (D). Values are normalized to IF in neurons of either genotype with basal activity.

G Overexpressed GFP-Bassoon but not EGFP reduces the nuclear localization and increases the cytoplasmic localization of endogenous CtBP1 in COS7 cells. Cells were stained for CtBP1 and with DAPI. Colored images show overlay.

H Quantification of nuclear IF of CtBP1 in COS7 cells expressing GFP-Bassoon or EGFP. The values are normalized to non-transfected cells (dashed line).

Data information: In all graphs, numbers in brackets indicate numbers of analyzed cells derived from two (B, C, E and F) or three independent cultures (H). One-way ANOVA with Bonferroni *post hoc* test (E, F and H) or Student's *t*-test (B and C) was used for statistics: ns, $P > 0.05$; *$P < 0.05$;***$P < 0.001$. All scale bars are 10 μm.

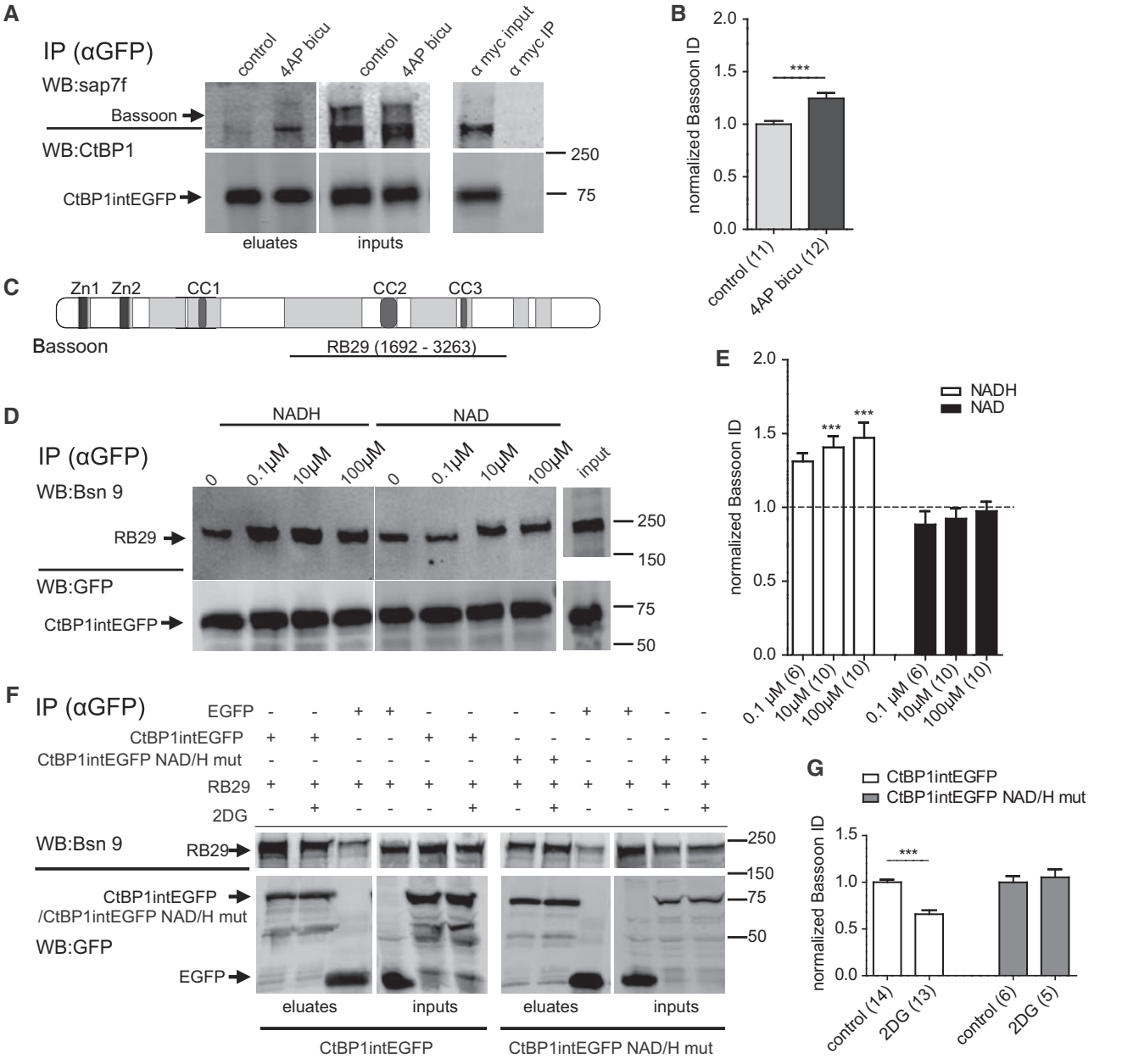

Figure 8. NADH concentration controls interaction of CtBP1 with Bassoon.

A Enhanced activity stimulates Bassoon–CtBP1 interaction. Co-IP with GFP antibodies was performed from neurons expressing CtBP1intEGFP at basal or elevated (4AP bicu, 30 min) activity. Precipitation with antibody against myc was used as a control for the specificity of binding.

B Quantification of Bassoon immunoreactivity in a complex with CtBP1intEGFP normalized to co-IP from neurons with basal activity in (A).

C Extent of RB29 on rat Bassoon sequence. Zn1,2, zinc fingers; CC, coiled coil regions; gray boxes show the regions of high Bassoon–Piccolo homology. Numbers indicate corresponding aa residues.

D Co-IP (using a GFP-specific antibody) of RB29 with CtBP1intEGFP from transfected HEK293T cells. Effect of increasing NADH and NAD concentration on co-IP of RB29 with CtBP1intEGFP.

E Quantifications of increasing NAD and NADH concentrations on co-IP of RB29 with CtBP1intEGFP. A ratio between RB29 in co-IP and CtBP1intEGFP in IP was calculated and normalized to the co-IP in control conditions (0 μM NAD or NADH).

F 2DG treatment reduces the co-IP of RB29 with CtBP1intEGFP but has no effect on RB29-CtBP1intEGFP NAD/H mutant co-IP. Control co-IP performed from cells expressing EGFP only showed some unspecific binding of RB29 to beads, which was, however, tenfold lower than the one of RB29 to CtBP1intEGFP.

G Quantifications of the effect of 2DG treatment on the co-IP of RB29 with CtBP1intEGFP or CtBP1intEGFP NAD/H mutant. The co-IP values were normalized to the co-IP in the control conditions.

Data information: The numbers in brackets (B, E and G) indicate the number of loadings of samples obtained in two to three independent experiments. Statistical analysis was done using Student's *t*-test (B, G) or one-way ANOVA with Bonferroni *post hoc* test (E): ns, $P > 0.05$; ***$P < 0.001$.
Source data are available online for this figure

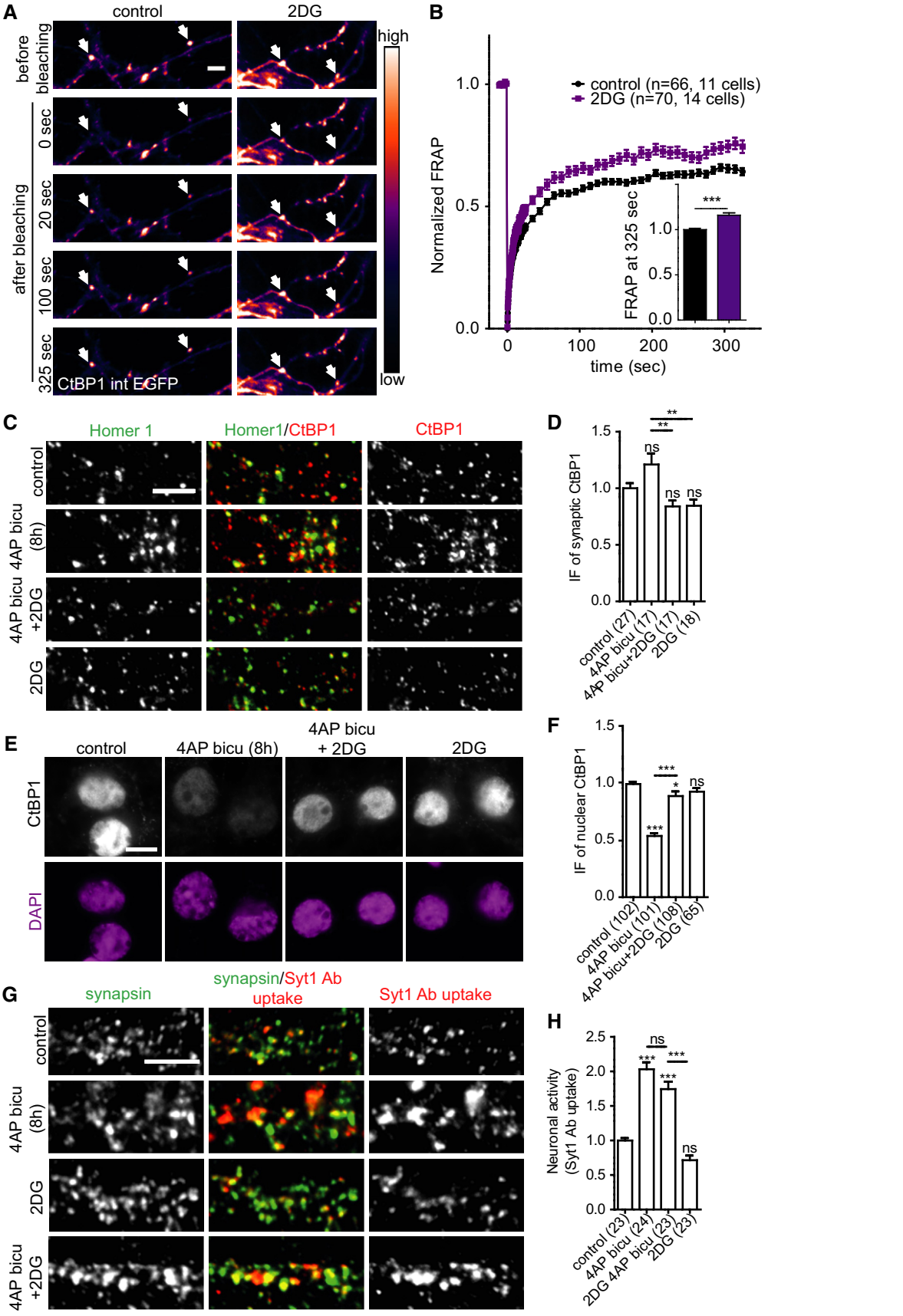

Figure 9.

Figure 9. Neuronal NAD/NADH balance controls the molecular dynamics of synaptic CtBP1 and its activity-induced nuclear shuttling.

A Fluorescence recovery after photobleaching (FRAP) of synaptic CtBP1intEGFP in control and 2DG-treated hippocampal neurons. Arrows indicate bleached synapses.

B Averaged FRAP traces for synapses in the experiment described in (A). Inserted plot shows a quantification of FRAP at 325 s after bleaching. Values are normalized to FRAP in control cultures.

C, D Staining of CtBP1 in synapses of neurons in cultures with basal or elevated activity and with or without 2DG treatment. Homer staining was used to mark synapses, DAPI stain for nuclei. Colored image shows overlay. Quantification of synaptic CtBP1 IF is shown in (D).

E, F Staining of CtBP1 in nuclei of neurons in cultures with basal or elevated activity and with or without 2DG treatment. Homer staining was used to mark synapses, DAPI stain for nuclei. Colored image shows overlay. Quantification of nuclear CtBP1 IF is shown in (F).

G Syt1 Ab uptake was used to evaluate the neuronal activity in untreated and 4AP bicu- and/or 2DG-treated neuronal cultures. Synapses were marked by staining for synapsin. Colored images show overlay.

H 4AP bicu treatment enhances the neuronal network activity to the same extent in control and 2DG-treated neuronal cultures as evaluated by Syt1 Ab uptake.

Data information: In graphs, numbers in brackets indicate the numbers of analyzed synapses (B), visual fields (E, H), or cells (F) and are derived from two (B, E and F) and three independent cultures (H). One-way ANOVA with Bonferroni *post hoc* test (E, F, H) or Student's *t*-test (B) was used for statistics: ns, $P > 0.05$; *$P < 0.05$; **$P < 0.01$, ***$P < 0.001$. Scale bars are 5 μm (A, C and G) and 10 μm (D).

NADH ratio upon elevation of neuronal activity in our preparation (Supplementary Fig S6B), which is in agreement with previous reports on tight coupling of cellular redox status to changes in neuronal activity (Kasischke *et al*, 2004; Brennan *et al*, 2006). Does the cellular metabolic state contribute to the activity-induced redistribution of CtBP1 between synapses and nucleus? To assess this, we tested whether neuronal activity influences the nuclear shuttling and the synaptic levels of CtBP1 in neurons after NADH depletion by 2DG treatment (Fig 9C–F). A long-term inhibition of glycolysis (2DG, 10 mM, 23 h) slightly, but not significantly, reduced the synaptic levels of CtBP1 and the synaptic activity monitored by Syt1 Ab uptake (Fig 9C, D, G and H, 71 ± 6.7% of control). Activity enhancement in 2DG-treated cultures induced an increased Syt1 Ab uptake indistinguishable from parallel cultures without the treatment (Fig 9G and H, normalized to Syt1 Ab uptake in cultures with basal activity: 4AP bicu: 200 ± 10%, 4AP bicu 2DG: 174 ± 11%), but it fully interfered with the increase of the synaptic CtBP1 upon activity enhancement (Fig 9C and D; 4AP bicu: 121 ± 9.8% of control; 2DG: 85 ± 5.6% of control; 4AP bicu 2DG: 84 ± 5.2% of control). Consistently, 2DG treatment also blocked the nuclear reduction of CtBP1 (Fig 9E and F; 4AP bicu: 54 ± 2.3% of control; 2DG: 93 ± 3.2% of control; 4AP bicu 2DG: 91 ± 2.7% of control).

Altogether, the presented here data show that the cellular NAD/NADH ratio critically influences the synaptic retention of CtBP1, presumably by regulation of the affinity to its synaptic anchors Bassoon and Piccolo. Moreover, the activity-induced depletion of nuclear CtBP1, which is diminished in absence of Bassoon and Piccolo (Fig 7D–F), is also highly sensitive to a depletion of the cellular NADH (Fig 9E and F). This strongly suggests that CtBP1-mediated transcriptional repression might be remotely controlled by modulation of the presynaptic targeting and retention of CtBP1 via its NADH-regulated interaction with the presynaptic scaffolding proteins Bassoon and Piccolo.

Discussion

Here we demonstrate that the transcriptional co-repressor CtBP1 is involved in the transcriptional control of activity-regulated genes in neurons and that its synapto-nuclear distribution, which is regulated by neuronal activity, plays an important role in this process. Furthermore, we have shown that the presynaptic proteins Bassoon and Piccolo bind to CtBP1 and mediate its recruitment to presynapse. This interaction is activity- and NADH-regulated and interferes with the nuclear translocation of CtBP1, which is in turn required for activity-driven expression of neuronal genes. Thus, our study reveals a mechanism, which could couple activity-induced molecular reorganization in presynapses to regulation of cellular gene expression.

Neuronal activity regulates CtBP1 in the nucleus and at synapses: communication between the two cellular pools of CtBP1

CtBP1 occurs in two major confined pools in brain and cultured neurons: in the nucleus and in the presynaptic compartment (tom Dieck *et al*, 2005; Jose *et al*, 2008; Hubler *et al*, 2012). In addition, a soluble cytoplasmic CtBP1 pool has to be considered. While the nuclear localization corresponds to the well-established ubiquitous role of CtBP1 in the transcriptional regulation, the function of the presynaptic pool is currently unclear. Our data show that neuronal activity controls the amounts of CtBP1 in the nucleus and at the synaptic sites, most likely by redistribution between the two major pools. The molecular dynamics of synaptic CtBP1 were rapidly (within tens of minutes) modified by the ongoing synaptic activity, arguing for a regulation of its presynaptic retention by activity. Can CtBP1 once liberated from presynapses reach the cytoplasmic pool in the soma to possibly participate in its nucleo-cytoplasmic shuttling? The imaging of photoactivatable CtBP1 in living neurons supports this view and revealed a physical retrograde translocation of CtBP1 from distal neurites (presumably presynapses) to soma. Retrograde transport of neurotrophin-induced signaling endosomes or injury signaling from lesion sites to cell bodies are the best studied examples of long-distance signaling from presynapses and axons to nucleus (Fainzilber *et al*, 2011). Translocation of signaling molecules from neurites to nucleus can be mediated by active transport mechanisms (Hanz *et al*, 2003; Wu *et al*, 2007) or by facilitated diffusion (Wiegert *et al*, 2007). In our experiments, CtBP1 photoactivated at synapse appears in the nucleus in the time frame of hours suggesting an involvement of slow axonal transport or facilitated diffusion. The exact mode and the molecular machinery mediating the retrograde translocation of CtBP1 in neurons call for future studies.

Shuttling of CtBP1 between cytoplasm and nucleus was investigated in numerous studies in non-neuronal cells (Riefler & Firestein,

2001; Barnes *et al*, 2003; Lin *et al*, 2003; Verger *et al*, 2006). Here, the amount of nuclear CtBP1 is determined by the rate of its nuclear import (which occurs only via binding to NLS-containing proteins) and export, likely driven by a putative NES present in CtBP1 (Verger *et al*, 2006). Our experiments in neurons indicate a relatively low export rate for CtBP1 under basal neuronal activity, while elevation of the network activity induced its rapid exportin-dependent nuclear depletion. Several mechanisms might account for this, including a control at the level of retention in chromatin-associated complexes, at the export level by modulation of its association with exportins or at the level of nuclear import by regulating the association of CtBP1 with NLS-containing factors. Supporting the last option, increasing NADH concentrations (occurring upon elevation of neuronal activity) promote binding of Bassoon to CtBP1, which mediates synaptic targeting/retention of CtBP1, while in the same time reduce binding of CtBP1 to NRSF or p300, the nuclear regulators functionally associated with CtBP1 (Kim *et al*, 2005; Garriga-Canut *et al*, 2006). Thus, neuronal activity might modulate the subcelullar distribution and the co-repressor activity of CtBP1 by controlling its association with compartment-specific interaction partners.

Nucleo-cytoplasmic shuttling of CtBP1 controls expression of activity-regulated genes

Shuttling between the cytoplasmic and the nuclear compartment is one of the most important means of regulation of the co-repressor activity of CtBP1 in non-neuronal cells (Riefler & Firestein, 2001; Barnes *et al*, 2003). In this study, we identified a number of activity-regulated genes as targets of the transcriptional control of CtBP1 in neurons. Among them, *BDNF* gene was previously reported to be repressed by CtBP1/NRSF protein complex (Garriga-Canut *et al*, 2006; Hara *et al*, 2009). New targets of CtBP1 identified here include genes coding for transcription factors: c-Fos and jun-B, the activity-regulated cytoskeleton-associated protein ARC/ARG3.1, signaling molecules: a subunit of CaM kinase II and cGMP-dependent protein kinase 1, neurotrophins: EGR1, EGR4, NT-3, and NT-4, neurotrophin receptor p75 NGF receptor, neurotransmitter receptor subunits such as the GluN2A-subunit of the NMDA receptor, the α5-subunit of $GABA_A$ receptors or the mGluR2 metabotropic glutamate receptor. Modulation of neuronal activity, which normally affects the expression of a subset of these genes, had no or only minor effect in cells depleted from endogenous CtBP1. At the same time, block of nuclear export, which severely interfered with the expressional regulation of these genes by neuronal activity, had a significantly lower effect in neurons depleted from CtBP1. This implies that CtBP1 and more specifically its activity-induced shuttling between nucleus and cytoplasm are required for normal induction of activity-regulated genes by neuronal activity. In this respect, CtBP1 is strongly reminiscent of previously described nuclear factors that shuttle between nucleus and cytoplasm in an activity-dependent manner (Jordan & Kreutz, 2009; Ch'ng & Martin, 2011). Important to note, most of these synapse-to-nucleus messenger molecules were implied and studied in context of spine to nucleus signaling. In contrast, CtBP1 is a shuttling nuclear factor specifically localized in the presynaptic compartment (tom Dieck *et al*, 2005; Hubler *et al*, 2012). Activity-dependent reconfiguration of gene expression occurs on timescales from minutes to days. While the induction of some of the immediate early genes takes place within minutes upon the stimulus onset and is dependent on back-propagating action potentials or somatic/nuclear Ca^{2+} waves, the expressional control mediated by CtBP1 (and other activity-regulated synapse-to-nucleus messengers) occurs at a longer timescale (within hours) and might therefore play an important role in long-term modifications of gene expression during memory formation, homeostatic plasticity or adaptive plasticity.

CtBP1 exerts its nuclear role as a part of a repressor complex, which can contain also class II histone deacetylases (HDACs). Neuronal activity-triggered shuttling of HDACs II occurs in a time frame comparable to what we observed for CtBP1 (Chawla *et al*, 2003; Schlumm *et al*, 2013; Soriano *et al*, 2013). Decisive for shuttling of HDACs II are activity-evoked somatic Ca^{2+} waves originating upon depolarization of the dendritic compartment (Chawla *et al*, 2003). Interestingly, block of somatic calcium channels does not interfere with the activity-dependent shuttling of CtBP1 (data not shown), suggesting that diverse signaling pathways converge to regulate gene expression via nuclear CtBP1-based repressor complex. Considering its presynaptic localization (Hubler *et al*, 2012), transcriptional repression by CtBP1 might also play a role in integration of dendritic and axonal signals and result in specific regulation of gene expression dependent on the activity of entire brain circuits.

Bassoon and Piccolo are key players in regulating neuronal distribution of CtBP1 in neurons

Bassoon and Piccolo are required for normal synaptic localization of CtBP1; upon deletion of both proteins, no CtBP1 could be found in synapses. The interaction occurs via the substrate-binding domain of CtBP1 and PXDLS-based motifs of Bassoon and Piccolo, analogously to the binding of CtBP1 to the NLS-containing factors (e.g. BKLF) mediating its nuclear import (Quinlan *et al*, 2006; Verger *et al*, 2006). Bassoon and Piccolo are synthesized in the soma of neurons, undergo a *trans*-Golgi-dependent trafficking step, and are transported toward synapses on the cytoplasmic surface of membranous organelles, PTVs (Zhai *et al*, 2001; Dresbach *et al*, 2006). CtBP1 seems to bind Bassoon already during its trafficking as we could show its association with PTVs. Hence, we propose that Bassoon and Piccolo trap cytoplasmic and axonal CtBP1, direct it to the presynaptic compartment and thereby compete with its nuclear binding partners and remotely control transcriptional repression by regulation of the availability of CtBP1 for nuclear import. In line with this, Bassoon ectopically expressed in non-neuronal cells sequestered endogenous CtBP1, which led to an enhanced cytoplasmic and a reduced nuclear localization of CtBP1. Vice versa, CtBP1 accumulated in the nucleus in absence of Bassoon and Piccolo and CtBP1-mediated repression was enhanced. While evoked and spontaneous synaptic transmission were reported to be normal in neurons deficient for both Piccolo and Bassoon in a previous study (Mukherjee *et al*, 2010), we found a reduced Syt1 Ab uptake driven by endogenous network activity (Supplementary Fig S5). This suggests a lower basal network activity in DKO, which might contribute to the increased nuclear CtBP1 abundance in these neurons. Nevertheless, network activity silencing or enhancement failed to induce nuclear shuttling of CtBP1 in DKO neurons, implying that loss of the synaptic anchor of CtBP1 interferes with its

normal activity-induced translocation. Furthermore our results indicate that the sensitivity of Bassoon–CtBP1 binding to changes in the NADH concentrations underlies the activity-dependent modulation of the synaptic anchoring of CtBP1. Interestingly, block of glycolysis by 2DG prevented the activity-induced depletion of nuclear CtBP1 and facilitated its dynamics at presynapse. We hypothesize that 2DG-induced reduction in the NADH levels hampered the synaptic retention of CtBP1 due to its dissociation from Bassoon/Piccolo, which made more CtBP1 available for replenishment of its nuclear pool. We believe that multiple mechanisms regulating the nuclear import and export of CtBP1, as in non-neuronal cells, will also play a role in neurons and must be revisited in future studies. Nonetheless, we demonstrate here that Bassoon/Piccolo-mediated trapping and synaptic anchoring of CtBP1 importantly expands the mode of CtBP1 transcriptional regulation in neurons. This novel role of Bassoon and Piccolo in regulation of CtBP1 subcellular localization links these large presynaptic scaffolds to the transcriptional control of neuronal activity-regulated genes.

Materials and Methods

Antibodies

The following antibodies were used in the study: mouse antibodies against CtBP1 [immunocytochemistry (ICC) 1:1,000, Western blotting (WB) 1:5,000; BD Transduction Laboratories], synaptophysin (SVP-38, WB 1:1,000; Sigma), Bassoon (mab7f, WB 1:2,000; Assay Designs), and β-actin (WB 1:2,000; Sigma), Homer1 (ICC 1:500; Synaptic Systems); rabbit antibodies against Homer1 (ICC 1:500, WB 1:1,000; Synaptic Systems), Bassoon (sap 7f, ICC 1:1,000, WB 1:1,000; tom Dieck *et al*, 1998), GFP (ICC 1:1,000, WB 1:5,000, ab 6556; Abcam), GAPDH (WB 1:3,000; Abcam), and GST (WB 1:10,000; Covance); and guinea pig antibodies against synaptophysin 1 (ICC 1:1,000, WB 1:1,000; Synaptic Systems), synapsin 1, 2 (ICC 1:1,000, WB 1:1,000; Synaptic Systems), Bassoon–Bsn9 (WB 1:1,000, sera generated by immunization with purified GST-tagged fragment covering amino acid residues 2,613–2,774 of rat Bassoon), and Piccolo (ICC 1:1,000; Dick *et al*, 2001). Alexa 488- (ICC: 1:1,000), Cy3-(ICC: 1:1,000), Cy5-(ICC: 1:2,000), and peroxidase-coupled antibodies (1:10,000) were purchased from Jackson ImmunoResearch Laboratories, Alexa 680 (WB 1:20,000) from Invitrogen/ Molecular Probes, IRDye™ 800CW (WB 1:20,000) from Rockland, Abberior STAR 580 (1:100) from Abberior GmbH, and Atto 647N (1:500) from Atto-Tec GmbH.

Animals

Wistar rats, Bassoon ($Bsn^{-/-}$) (Frank *et al*, 2010; Hallermann *et al*, 2010) and Piccolo (Pclo3) mouse strains backcrossed to C57BL/6N were used to obtain tissues and cells used in this study. $Bsn^{-/-}$ mice were obtained from Omnibank ES cell line OST486029 by Lexicon Pharmaceuticals, Inc. (The Woodlands, TX, USA). Pclo3 constitutive mutant strain was obtained by crossing of $Pclo^{tm2Sud}$/J conditional mutant strain (Jacson Laboratory; Mukherjee *et al*, 2010) with the ubiquitously expressing Cre line Tg(CMV-Cre)1Nagy (Nagy *et al*, 1998). All experiments were carried out in accordance with the European Committees Council Directive (86/609/EEC) and approved by the local animal care committee (Landesverwaltungsamt Sachsen-Anhalt, AZ: 42502/2-988 IfN).

DNA constructs

We used CtBP1-S (NM_019201.3, NP_062074.2) for all expression studies in this work. CtBP1intEGFP was generated by insertion of the EGFP or the photoactivatable EGFP (PAEGFP) sequences between amino acids 361 and 362 of CtBP1. CtBP1int(PA)EGFP was expressed from pCMV or FUGW lentiviral vector. Piccolo fragments RP1–5 and 16 (Fig 5A) were generated by PCR using the pACT2 rat brain Matchmaker cDNA library (Clontech Laboratories, Inc.) as a template. For RP10, 11 and 13–15 corresponding oligonucleotides were synthesized and used for cloning. pBDNFpI+II (Hara *et al*, 2009) was subcloned upstream of EGFP in FUGW (Lois *et al*, 2002) lentiviral transfer vector. For yeast two-hybrid (Y2H) analysis, Bassoon fragment RB46 and all Piccolo fragments in pGBKT7 and CtBP1 (and its mutants targeting substrate-binding pocket) in pGADT7 were used (tom Dieck *et al*, 2005). For pull-down assays, bacterially expressed 6xHis-tag thioredoxin fusion proteins were generated by expression the Piccolo fragments from pET32a(+) (Novagen). Glutathione S-transferase (GST)-CtBP1 fusion proteins were expressed from pGEX-5X-1 (Amersham Pharmacia Biotech). GFP-Bsn (amino acids 95-3,938) and RB29 were described previously (Dresbach *et al*, 2003; tom Dieck *et al*, 2005). All constructs were verified by sequencing.

shRNAs design and cloning

Four independent shRNAs were designed using online available shRNA designing tools from Ambion and Promega; two of them having highest efficiency were used in this study: shRNA944: covering nucleotides (nt) 944–962, and shRNA467: nt 467–485 of rat CtBP1 (NM_019201.2). As scrambled control the following sequence was used: GACTTTACTGCCCCTTACT. All shRNAs contain TTCAAGAGA loop sequence. shRNAs were inserted into pZOff, and then, H1 expression cassettes were cloned into the lentiviral transfer vector FUGW H1 as described previously (Leal-Ortiz *et al*, 2008). CtBP1intEGFPCtBP1KD944 and EGFP-CtBP1CtBP1KD944 bi-cistronic vectors were created by replacing the EGFP sequence in FUGW H1, containing shRNA944, with CtBP1intEGFP or EGFP-CtBP1 sequences carrying four silent point mutations in the target sequence for shRNA944. The shRNA against Piccolo (Pclo28) was previously described (Leal-Ortiz *et al*, 2008).

Y2H analysis

For Y2H analysis, each Bassoon or Piccolo fragment in pGBK-T7 was co-transformed with CtBP1 in pGAD-T7 into AH109 yeast cells (CLONTECH Laboratories, Inc.) using standard transformation protocols. Co-transformed cells were selected by growth on leucine- and tryptophan-lacking medium and were assayed for reporter gene expression by growth on leucine-, tryptophan-, adenine-, and histidine-lacking medium in the presence of 1 mM 3-amino-1,2,4-triazole. Growth was monitored and scored after 7–10 days. Potential self-activation of constructs was always tested in parallel by co-transformation with empty prey or bait vectors.

Lentiviral particle production

Lentiviral particles were produced in HEK293T cells (ATTC, Manassas, VA, USA) using three vectors: FUGW-based transfer, psPAX2 packaging, and pVSVG pseudotyping vectors (Lois *et al*, 2002). HEK293T cells were grown in media containing 10% fetal bovine sera (FBS) to 80% confluence and transfected (on day 1) using the calcium phosphate method as described earlier (Fejtova *et al*, 2009). Molar ratio of FUGW:psPAX2:pVSVG was 2:1:1. On day 2, FBS content was reduced to 4%. On day 3 and 4, the virus-containing media were collected, cleared by passing through 0.45-μm filter, and then concentrated via ultracentrifugation for 2 h at 100,000 *g*. The viral particles were resuspended in NB medium, containing B27, antibiotics, and 0.8 mM glutamine, aliquoted, and stored at −80°C.

Primary neuronal cultures, transfections, viral infections, and treatments

Primary hippocampal cultures from rats and cultures from rat cortex neurons were prepared as described earlier (Frischknecht *et al*, 2008; Lazarevic *et al*, 2011), respectively. For culturing of primary hippocampal neurons from mice, newborn animals of desired genotype and their wild-type siblings were killed by decapitation, their brains were removed, and hippocampi were freed of meninges. The cell suspension obtained after 0.025% trypsin treatment and mechanical trituration was plated in DMEM supplemented with 10% FBS, 1 mM glutamine and antibiotics (100 U/ml penicillin, 100 μg/ml streptomycin) onto poly-L-lysine (Sigma)-coated round glass coverslips (30,000 cells; 18 mm diameter). After 1 h, coverslips were transferred into dishes containing 70–80% confluent monolayer of astrocytes and Neurobasal A medium supplemented with B27, 1 mM sodium pyruvate, antibiotics (100 U/ml penicillin, 100 μg/ml streptomycin) and 4 mM GlutaMax. At DIV (day *in vitro*) 1, AraC was added to the cells to the final concentration of 0.6 μM; additional AraC was applied at DIV 3 to reach the final concentration of 1.2 μM. GFP-Bassoon was expressed as described previously (Fejtova *et al*, 2009). For shRNA-mediated knockdown of CtBP1, the cultures were transduced with lentiviral particles with nearly 100% efficiency of transduction, on the day of plating (DIV 0), and cells were subjected to fixation or lyses after 2 weeks (DIV 14–16). For the live imaging experiments (FRAP and photoactivation), cultures were transduced at 5–7 DIV with high titer resulting in nearly 100% efficiency. For Fig 2B and C, low titer was used to obtain about 10–50 transduced cells per coverslip. Experiments were performed at DIV 16–20. In all cases, concentrated virus solution was added to neuronal growth media. For the treatments, the following pharmaceutics were used: tetrodotoxin (TTX, 2 μM; Tocris), D-(-)-2-amino-5-phosphonopentanoic acid (APV, 50 μM; Tocris), 6-cyano-7-nitroquinoxaline-2,3-dione disodium (CNQX, 10 μM; Tocris), 4-aminopyridine (4AP, 100 μM or 2.5 mM; Sigma-Aldrich), bicuculline (bicu, 50 μM; Sigma-Aldrich), leptomycin B (LB, 3 nM; Merck-Millipore), 2-deoxyglucose (2DG, 5 or 10 mM; Sigma-Aldrich), MG132 (10 μM; Sigma-Aldrich), lactacystin (Lacta, 0.5 μM; Merck-Millipore), and anisomycin (Aniso, 10 μM; Sigma-Aldrich). All chemicals used for neuronal cultures were obtained from Invitrogen, unless indicated otherwise.

Immunocytochemistry, wide-field, confocal, and STED microscopy, and image analysis

Immunostainings of neurons were done as described earlier (Lazarevic *et al*, 2011). For quantitative assessment, all coverslips compared in one experiments were processed in parallel using identical antibodies solutions and other reagents.

For the live staining with synaptotagmin 1 antibody (Syt1 Ab uptake), cells were incubated with fluorescence-labeled primary antibody dissolved in extracellular solution, containing 119 mM NaCl, 2.5 mM KCl, 2 mM $CaCl_2$, 2 mM $MgCl_2$, 30 mM glucose, and 25 mM HEPES, pH 7.4 for 30 min at 37°C (Kraszewski *et al*, 1995; Lazarevic *et al*, 2011). In order to prevent unspecific labeling, cells were washed two times with extracellular solution prior fixation or live imaging.

For the propidium iodide (PI) viability assay, control and 2DG-treated (5 mM, 48 h) cortical neurons were incubated with PI (5 μM) for 20 min at 37°C. The cells that served as a positive control were treated with 4% PFA for 10 min before the PI application. After washing two times with extracellular solution to remove unspecific PI labeling, cells were fixed, permeabilized, and stained with DAPI. The percentage of dead cells in each group was estimated as a ratio of the PI-positive cells versus the total number of cells, defined by the DAPI staining, in each visual field.

Images of stainings were acquired on a Zeiss Axio Imager A2 microscope with Cool Snap EZ camera (Visitron Systems) controlled by VisiView (Visitron Systems GmbH) software. Confocal image in Supplementary Fig S4A was obtained using a Leica SP5 confocal microscope (LAS AF software, version 2.0.2; 1024 × 1024 pixels display resolution, 12 bit dynamic range, 63× objective, NA 1.40, 3× optical zoom, pixel size approximately 60 nm). Confocal images in Supplementary Fig S4A and B were obtained using a Leica SP5 confocal microscope (LAS AF software, version 2.0.2; 1024 × 1024 pixels display resolution, 12 bit dynamic range, 63× objective, NA 1.40, 3× optical zoom, pixel size approximately 60 nm).

Dual-color STED images were acquired using Leica TCS-Sp5 Ti: Sapphire dual-color STED microscope (1024 × 1024 pixels display resolution, 8 bit dynamic range, 100× objective, NA 1.40, 6× optical zoom, pixel size app. 25 nm). Abberior STAR 580 and Atto 647N were excited using the setup pulsed-diode lasers (< 90 ps, 80 MHz, Pico Quant) at 531 and 635 nm, and detection was done at 589–625 and 655–685 nm, respectively. Depletion was done at 730 nm for the Abberior STAR 580 and at 750 nm for Atto 647N. Frames were acquired at a scan speed 700 Hz by applying 48 times line averaging. All acquired STED stacks were subsequently deconvolved using the Huygens professional (Scientific Volume Imaging, v 4.4.) STED package.

For quantifications, settings of camera or photomultiplier were applied identically to all coverslips quantified in one experiment. For each IF quantification in each experiment, images from at least three different coverslips were acquired and quantified to avoid effects given by experimental variance. Quantitative immunofluorescence (IF) analyses were performed using ImageJ (NIH, http://rsb.info.nih.gov/ij/) and OpenView software (Tsuriel *et al*, 2006). Threshold subtraction and measurements of nuclear IF were done in a mask created according to DAPI staining using NIH ImageJ. In all experiments, synaptic puncta were defined semi-automatically by

setting rectangular regions of interest (ROI) with dimensions about 0.8 × 0.8 μm around local intensity maxima in channel with staining for synaptic marker Homer 1, synaptophysin, or synapsin using OpenView software. Mean IF intensities were measured in nuclear and synaptic ROIs in all corresponding channels using the same software and normalized to the mean IF intensities of the control group for each of the experiments. Pearson's correlation coefficient in Fig 3B was calculated from the numeric values of the IF intensities for CtBP1intEGFP puncta before bleaching and the corresponding FRAP of the puncta at 325 s after bleaching; in Fig 4B, it was calculated from the numeric values of the IF intensities for CtBP1 and FEGFP expression (driven by BDNFpI+II) in ROIs determined by the DAPI staining in individual cells, using GraphPad Prism 5.

Quantitative real-time PCR

Primary cortical neuronal cultures were lysed at DIV 16, and total RNA was isolated with RNeasy Plus Mini Kit (Qiagen) according to the manufacturer's protocol. The transcripts were analyzed using Rat Synaptic Plasticity RT^2 Profiler PCR Array (Qiagen) or a customized version of the array and Roche LightCycler 480 according to manufacturer's instructions. The relative transcript levels of all investigated genes were normalized to the RNA amounts of hypoxanthine phosphoribosyltransferase 1 and lactate dehydrogenase A. The expression of the target genes in relation to the reference genes was calculated using ΔΔCP method. The crossing point (CP) of the PCR was determined by the 'second derivative maximum analysis' method, available in the software of Roche LightCycler480. For the rescue experiments in Fig 5B and C, total RNA was isolated from DIV 16 cortical cultures infected on the day of plating with scrambled, shRNA944 or CtBP1intEGFPCtBP1KD944, and EGFP-CtBP1 CtBP1KD944 lentiviral vectors. The relative transcript levels of BDNF and Arc were normalized to the RNA amounts of lactate dehydrogenase A.

Co-immunoprecipitation (co-IP) from HEK293T cells and from neurons

HEK293T cells were transfected using calcium phosphate method (Fejtova *et al*, 2009). Two days after the transfection, the cells were lysed for 5 min at 4°C in 50 mM Tris–HCl, pH 7.4, 0.5% Triton X-100, 10% glycerol, 100 mM NaCl, 1.5 mM MgCl containing complete protease inhibitors (Roche), and PhosStop (Roche) and cleared by centrifugation. The co-IPs were performed using MicroMACS anti-GFP MicroBeads and MicroColumns (Miltenyi Biotec) according to the manual from the manufacturer, except for the washing steps where the lyses buffer was used.

Cortical neurons grown in 75-cm^2 flasks were infected on DIV 5–7 with lentiviral particles, driving the expression of CtBP1intEGFP. Cells were lysed in ice-cold 10 mM Tris–HCl, 150 mM NaCl, 2% SDS, 1% deoxycholate and 1% Triton X-100 containing complete protease inhibitors (Roche), and PhosStop (Roche) 10 days later. Lysates were cleared by centrifugation at 1,000 *g* for 5 min. Detergent-insoluble fractions were pelleted by centrifugation at 12,000 *g* for 25 min and resuspended in the lysis buffer, and co-immunoprecipitations were performed using MicroMACS anti-GFP MicroBeads and MicroColumns (Miltenyi Biotec) following the manual from the manufacturer. In the detergent-soluble fractions, no co-immunoprecipitation of the endogenous Bassoon with CtBP1int EGFP was detected.

Isolation of PTVs and SVPs

Piccolo–Bassoon transport vesicles and SVPs were isolated exactly as described by Fejtova *et al* (2009).

Pull-down assays

Bacterial expression of His–Trx and GST fusion proteins in BL21-CodonPlus (DE3)RIPL (Stratagene) as well as affinity purification on Talon Metal affinity resin (BD Clontech) or Glutathion Sepharose CL4B (Amersham Pharmacia Biotech) were done according to the manufacturers' protocols. Purity and integrity of the purified fusion proteins were assessed on Coomassie-stained gels. His–Trx fusion proteins were coupled onto CNBr-activated Sepharose 4B (Amersham Biosciences) in a ratio of 1.25 mg protein per 250 μl bed volume of beads according to the manufacturers' protocol. Successful coupling was evaluated by protein concentration measurements of the protein containing solution before and after coupling procedure. In pull-down experiments, 20 μl of His–Trx fusion protein-coupled beads was incubated with GST-CtBP1 or GST at a concentration of 0.1 μg/μl for 1 h at 4°C in 1 ml of binding buffer [2.68 mM KCl, 1.47 mM KH_2PO_4, 8.06 mM Na_2HPO_4, 136.9 mM NaCl, 0.1% Tween-20 (pH 7.4)]. Beads were washed, and proteins were eluted in 90°C warm SDS–PAGE sample buffer.

Western blotting and quantification

Protein samples were separated using one-dimensional sodium dodecyl sulfate polyacrylamide gel electrophoresis (SDS–PAGE). For the detection of Bassoon fragment RB29 and CtBP1intEGFP, 5–20% Tris-glycine gels or 3.5–8% Tris-acetate gels were used. Detection of the endogenous CtBP1 and quantification of the expression levels of proteins was performed with 5–20% Tris-glycine gels. Proteins were then transferred to Millipore Immobilon-FL PVDF membranes by tank blotting. Immunodetection was performed with Hyperfilm ECL films (GE Healthcare) or using Odyssey Infrared Scanner (LI-COR). Quantitative immunoblots were obtained using Odyssey Infrared Scanner (LI-COR). Integrated density (ID) of signals was measured using ImageJ by setting rectangular ROIs around the bands, which had identical dimensions within each experimental group analyzed on the same membrane. Values were normalized to respective loading controls (GAPDH in Fig 1D, Supplementary Figs S3 and S4, and β-actin in Fig 6E) and to the average value of the control group for each individual membrane. In figures, Mw of markers are given in kDa and antibodies used for immunodetection on Western blots (WB) are indicated.

Imaging of fluorescence recovery after photobleaching and photoactivation

All live imaging experiments were performed at 37°C in extracellular solution, containing 119 mM NaCl, 2.5 mM KCl, 25 mM Hepes, pH 7.4, 30 mM glucose, 2 mM $MgCl_2$ and 2 mM $CaCl_2$, on inverted microscope (Observer. D1; Zeiss) equipped with an EMCCD camera (Evolve 512; Photometrics) controlled by MetaMorph Imaging (MDS

Analytical Technologies) and VisiView (Visitron Systems GmbH) software, using 63× objective and EGFP ET filter set (exciter 470/40, emitter 525/50, dichroic 495 LP) or DAPI/FITS/Texas Red filter set (exciter 407/494/576, emitter 457/530/628, dichroic 436/514/604) (Chroma Technology Corp.). The FRAP experiments were performed as previously described (Schroder *et al*, 2013). In detail, the FRAP targeting device Visifrap 2D (Visitron Systems GmbH) was driving the FRAP laser DL-473 (Rapp Optoelectronics) or the photoactivation laser (VS-SLS Single-Laser-System; Visitron System GmbH). In all FRAP experiments, 10 baseline images (1 Hz, 250-ms exposure) were collected before 6–10 puncta were bleached by high-intensity 473-nm laser pulse of 10 ms resulting on average in a $1.8 \pm 0.1\ \mu m^2$ bleached area. Then, 100 images at 4 Hz, 250 ms exposure, and 300 images at 1 Hz were acquired to monitor the recovery. The synaptic photoactivation was performed by delivering a laser pulse of 1 s in 50–100 circular ROIs with a radius of 1.87 μm set around Syt1 Ab staining, which was performed 30 min before the live imaging; nuclear photoactivation was performed by laser scanning (1-s laser pulse time) in a circular ROI set around the cell body. Images (250 ms exposure) were taken at time points as indicated in the main figures. All live imaging experiments were analyzed using ImageJ software. FRAP recovery rates were determined after background subtraction [from two individual regions of interest (ROIs) in the background] and were normalized to the intensity before photobleaching, set to 1, and to the first value after photobleaching, set to 0. Data were corrected for bleaching; a bleaching factor was estimated from the bleaching of the naive puncta on the same image. For the photoactivation experiments, the decline of the mean fluorescence intensities was measured in ROIs defined by the live staining with synaptotagmin 1 antibody. $F^{(PA)EGFP}$ at individual synapses at each time point (Ft) was normalized to the $F^{(PA)EGFP}$ in the first frame after photoactivation (F0). In FRAP and PA experiments, new coverslip was used for each bleaching or PA.

Analysis of the cellular NAD/NADH ratio

Quantitative determination of NAD and NADH concentrations in samples from primary cortical cultures (DIV 21) was performed using EnzyChrom™ NAD^+/NADH assay kit from BioAssay System according to the manual from the manufacturer.

Statistics

All results of quantitative analyses are given as means ± standard errors of the mean (SEM). Statistical analyses were performed with Prism 5 software (GraphPad Software, Inc.) using one-way ANOVA or Student's *t*-test as indicated for each experiment. Statistical significance is marked as $*P < 0.05$, $**P < 0.01$, $***P < 0.001$ in all plots. Information about group character and size is specified in figure legend for each experiment.

Supplementary information for this article is available online: http://emboj.embopress.org

Acknowledgements

We thank K. Hartung, J. Juhle, B. Kracht, A. Lenuweit, S. Opitz, and H. Wickborn for excellent technical support, A. Pellerito for help with quantifications, O. Kobler and SL ELMI for help with STED imaging, C.C. Garner for providing FUGWH1 and M. Fukuchi and M. Tsuda for pBDNF-PI+PIIwild in pGL3 vector, and all members of the Magdeburg laboratories for helpful discussions. The study was supported by DFG (SFB779/B9 and GRK 1167 to EDG; AL1115/1-1 to WDA and FE1335/1 to AF), ERANET Neuron (FKZ 01EW1101) to EDG, the Leibniz Association (SAW 2013-15) to AF and EDG, the Schram Foundation to RF, and by the Federal State of Saxony-Anhalt (CBBS, NeuroNetwork #5) to AF and DS.

Author contributions

DI, RF, EDG, and AF wrote the manuscript. DI, WDA, and AF conceived or designed the experiments. DI, AD, CS, WDA, and AF performed the experiments. DI, AD, CS, and WDA analyzed the data. CM-V and CM provided DKO mouse cultures. RF provided expertise in live imaging experiments. DS and MZ provided and supervised qPCR platform.

Conflict of interest

The authors declare that they have no conflict of interest.

References

Alabi AA, Tsien RW (2012) Synaptic vesicle pools and dynamics. *Cold Spring Harb Perspect Biol* 4: a013680

Barnes CJ, Vadlamudi RK, Mishra SK, Jacobson RH, Li F, Kumar R (2003) Functional inactivation of a transcriptional corepressor by a signaling kinase. *Nat Struct Biol* 10: 622 – 628

Brennan AM, Connor JA, Shuttleworth CW (2006) NAD(P)H fluorescence transients after synaptic activity in brain slices: predominant role of mitochondrial function. *J Cereb Blood Flow Metab* 26: 1389 – 1406

Chawla S, Vanhoutte P, Arnold FJ, Huang CL, Bading H (2003) Neuronal activity-dependent nucleocytoplasmic shuttling of HDAC4 and HDAC5. *J Neurochem* 85: 151 – 159

Chinnadurai G (2007) Transcriptional regulation by C-terminal binding proteins. *Int J Biochem Cell Biol* 39: 1593 – 1607

Chinnadurai G (2009) The transcriptional corepressor CtBP: a foe of multiple tumor suppressors. *Cancer Res* 69: 731 – 734

Ch'ng TH, Martin KC (2011) Synapse-to-nucleus signaling. *Curr Opin Neurobiol* 21: 345 – 352

Corda D, Colanzi A, Luini A (2006) The multiple activities of CtBP/BARS proteins: the Golgi view. *Trends Cell Biol* 16: 167 – 173

Dick O, Hack I, Altrock WD, Garner CC, Gundelfinger ED, Brandstatter JH (2001) Localization of the presynaptic cytomatrix protein Piccolo at ribbon and conventional synapses in the rat retina: comparison with Bassoon. *J Comp Neurol* 439: 224 – 234

Dick O, tom Dieck S, Altrock WD, Ammermuller J, Weiler R, Garner CC, Gundelfinger ED, Brandstatter JH (2003) The presynaptic active zone protein bassoon is essential for photoreceptor ribbon synapse formation in the retina. *Neuron* 37: 775 – 786

tom Dieck S, Sanmarti-Vila L, Langnaese K, Richter K, Kindler S, Soyke A, Wex H, Smalla KH, Kampf U, Franzer JT, Stumm M, Garner CC, Gundelfinger ED (1998) Bassoon, a novel zinc-finger CAG/glutamine-repeat protein selectively localized at the active zone of presynaptic nerve terminals. *J Cell Biol* 142: 499 – 509

tom Dieck S, Altrock WD, Kessels MM, Qualmann B, Regus H, Brauner D, Fejtova A, Bracko O, Gundelfinger ED, Brandstatter JH (2005) Molecular dissection of the photoreceptor ribbon synapse: physical interaction of Bassoon and RIBEYE is essential for the assembly of the ribbon complex. *J Cell Biol* 168: 825 – 836

Dresbach T, Hempelmann A, Spilker C, tom Dieck S, Altrock WD, Zuschratter W, Garner CC, Gundelfinger ED (2003) Functional regions of the presynaptic cytomatrix protein bassoon: significance for synaptic targeting and cytomatrix anchoring. *Mol Cell Neurosci* 23: 279 – 291

Dresbach T, Torres V, Wittenmayer N, Altrock WD, Zamorano P, Zuschratter W, Nawrotzki R, Ziv NE, Garner CC, Gundelfinger ED (2006) Assembly of active zone precursor vesicles: obligatory trafficking of presynaptic cytomatrix proteins Bassoon and Piccolo via a trans-Golgi compartment. *J Biol Chem* 281: 6038 – 6047

Fainzilber M, Budnik V, Segal RA, Kreutz MR (2011) From synapse to nucleus and back again–communication over distance within neurons. *J Neurosci* 31: 16045 – 16048

Fejtova A, Davydova D, Bischof F, Lazarevic V, Altrock WD, Romorini S, Schone C, Zuschratter W, Kreutz MR, Garner CC, Ziv NE, Gundelfinger ED (2009) Dynein light chain regulates axonal trafficking and synaptic levels of Bassoon. *J Cell Biol* 185: 341 – 355

Fenster SD, Chung WJ, Zhai R, Cases-Langhoff C, Voss B, Garner AM, Kaempf U, Kindler S, Gundelfinger ED, Garner CC (2000) Piccolo, a presynaptic zinc finger protein structurally related to bassoon. *Neuron* 25: 203 – 214

Frank T, Rutherford MA, Strenzke N, Neef A, Pangrsic T, Khimich D, Fejtova A, Gundelfinger ED, Liberman MC, Harke B, Bryan KE, Lee A, Egner A, Riedel D, Moser T (2010) Bassoon and the synaptic ribbon organize Ca(2)+ channels and vesicles to add release sites and promote refilling. *Neuron* 68: 724 – 738

Frischknecht R, Fejtova A, Viesti M, Stephan A, Sonderegger P (2008) Activity-induced synaptic capture and exocytosis of the neuronal serine protease neurotrypsin. *J Neurosci* 28: 1568 – 1579

Garriga-Canut M, Schoenike B, Qazi R, Bergendahl K, Daley TJ, Pfender RM, Morrison JF, Ockuly J, Stafstrom C, Sutula T, Roopra A (2006) 2-Deoxy-D-glucose reduces epilepsy progression by NRSF-CtBP-dependent metabolic regulation of chromatin structure. *Nat Neurosci* 9: 1382 – 1387

Greer PL, Greenberg ME (2008) From synapse to nucleus: calcium-dependent gene transcription in the control of synapse development and function. *Neuron* 59: 846 – 860

Hagenston AM, Bading H (2011) Calcium signaling in synapse-to-nucleus communication. *Cold Spring Harb Perspect Biol* 3: a004564

Hallermann S, Fejtova A, Schmidt H, Weyhersmuller A, Silver RA, Gundelfinger ED, Eilers J (2010) Bassoon speeds vesicle reloading at a central excitatory synapse. *Neuron* 68: 710 – 723

Hanz S, Perlson E, Willis D, Zheng JQ, Massarwa R, Huerta JJ, Koltzenburg M, Kohler M, van-Minnen J, Twiss JL, Fainzilber M (2003) Axoplasmic importins enable retrograde injury signaling in lesioned nerve. *Neuron* 40: 1095 – 1104

Hara D, Fukuchi M, Miyashita T, Tabuchi A, Takasaki I, Naruse Y, Mori N, Kondo T, Tsuda M (2009) Remote control of activity-dependent BDNF gene promoter-I transcription mediated by REST/NRSF. *Biochem Biophys Res Commun* 384: 506 – 511

Hubler D, Rankovic M, Richter K, Lazarevic V, Altrock WD, Fischer KD, Gundelfinger ED, Fejtova A (2012) Differential spatial expression and subcellular localization of CtBP family members in rodent brain. *PLoS One* 7: e39710

Jordan BA, Kreutz MR (2009) Nucleocytoplasmic protein shuttling: the direct route in synapse-to-nucleus signaling. *Trends Neurosci* 32: 392 – 401

Jose M, Nair DK, Altrock WD, Dresbach T, Gundelfinger ED, Zuschratter W (2008) Investigating interactions mediated by the presynaptic protein bassoon in living cells by Foerster's resonance energy transfer and fluorescence lifetime imaging microscopy. *Biophys J* 94: 1483 – 1496

Kasischke KA, Vishwasrao HD, Fisher PJ, Zipfel WR, Webb WW (2004) Neural activity triggers neuronal oxidative metabolism followed by astrocytic glycolysis. *Science* 305: 99 – 103

Katsanis N, Fisher EM (1998) A novel C-terminal binding protein (CTBP2) is closely related to CTBP1, an adenovirus E1A-binding protein, and maps to human chromosome 21q21.3. *Genomics* 47: 294 – 299

Khimich D, Nouvian R, Pujol R, tom Dieck S, Egner A, Gundelfinger ED, Moser T (2005) Hair cell synaptic ribbons are essential for synchronous auditory signalling. *Nature* 434: 889 – 894

Kim JH, Cho EJ, Kim ST, Youn HD (2005) CtBP represses p300-mediated transcriptional activation by direct association with its bromodomain. *Nat Struct Mol Biol* 12: 423 – 428

Kraszewski K, Mundigl O, Daniell L, Verderio C, Matteoli M, De Camilli P (1995) Synaptic vesicle dynamics in living cultured hippocampal neurons visualized with CY3-conjugated antibodies directed against the lumenal domain of synaptotagmin. *J Neurosci* 15: 4328 – 4342

Kumar V, Carlson JE, Ohgi KA, Edwards TA, Rose DW, Escalante CR, Rosenfeld MG, Aggarwal AK (2002) Transcription corepressor CtBP is an NAD(+)-regulated dehydrogenase. *Mol Cell* 10: 857 – 869

Kuppuswamy M, Vijayalingam S, Zhao LJ, Zhou Y, Subramanian T, Ryerse J, Chinnadurai G (2008) Role of the PLDLS-binding cleft region of CtBP1 in recruitment of core and auxiliary components of the corepressor complex. *Mol Cell Biol* 28: 269 – 281

Lazarevic V, Schone C, Heine M, Gundelfinger ED, Fejtova A (2011) Extensive remodeling of the presynaptic cytomatrix upon homeostatic adaptation to network activity silencing. *J Neurosci* 31: 10189 – 10200

Leal-Ortiz S, Waites CL, Terry-Lorenzo R, Zamorano P, Gundelfinger ED, Garner CC (2008) Piccolo modulation of Synapsin1a dynamics regulates synaptic vesicle exocytosis. *J Cell Biol* 181: 831 – 846

Lin X, Sun B, Liang M, Liang YY, Gast A, Hildebrand J, Brunicardi FC, Melchior F, Feng XH (2003) Opposed regulation of corepressor CtBP by SUMOylation and PDZ binding. *Mol Cell* 11: 1389 – 1396

Lois C, Hong EJ, Pease S, Brown EJ, Baltimore D (2002) Germline transmission and tissue-specific expression of transgenes delivered by lentiviral vectors. *Science* 295: 868 – 872

Mihaly A, Joo F, Szente M (1983) Neuropathological alterations in the neocortex of rats subjected to focal aminopyridine seizures. *Acta Neuropathol* 61: 85 – 94

Mukherjee K, Yang X, Gerber SH, Kwon HB, Ho A, Castillo PE, Liu X, Sudhof TC (2010) Piccolo and bassoon maintain synaptic vesicle clustering without directly participating in vesicle exocytosis. *Proc Natl Acad Sci USA* 107: 6504 – 6509

Nagy A, Moens C, Ivanyi E, Pawling J, Gertsenstein M, Hadjantonakis AK, Pirity M, Rossant J (1998) Dissecting the role of N-myc in development using a single targeting vector to generate a series of alleles. *Curr Biol* 8: 661 – 664

Nardini M, Spano S, Cericola C, Pesce A, Massaro A, Millo E, Luini A, Corda D, Bolognesi M (2003) CtBP/BARS: a dual-function protein involved in transcription co-repression and Golgi membrane fission. *EMBO J* 22: 3122 – 3130

Patterson GH, Lippincott-Schwartz J (2002) A photoactivatable GFP for selective photolabeling of proteins and cells. *Science* 297: 1873 – 1877

Quinlan KG, Verger A, Kwok A, Lee SH, Perdomo J, Nardini M, Bolognesi M, Crossley M (2006) Role of the C-terminal binding protein PXDLS motif binding cleft in protein interactions and transcriptional repression. *Mol Cell Biol* 26: 8202 – 8213

Riefler GM, Firestein BL (2001) Binding of neuronal nitric-oxide synthase (nNOS) to carboxyl-terminal-binding protein (CtBP) changes the

localization of CtBP from the nucleus to the cytosol: a novel function for targeting by the PDZ domain of nNOS. *J Biol Chem* 276: 48262 – 48268

Rylski M, Amborska R, Zybura K, Mioduszewska B, Michaluk P, Jaworski J, Kaczmarek L (2008) Yin Yang 1 is a critical repressor of matrix metalloproteinase-9 expression in brain neurons. *J Biol Chem* 283: 35140 – 35153

Schlumm F, Mauceri D, Freitag HE, Bading H (2013) Nuclear calcium signaling regulates nuclear export of a subset of class IIa histone deacetylases following synaptic activity. *J Biol Chem* 288: 8074 – 8084

Schmitz F, Konigstorfer A, Sudhof TC (2000) RIBEYE, a component of synaptic ribbons: a protein's journey through evolution provides insight into synaptic ribbon function. *Neuron* 28: 857 – 872

Schroder MS, Stellmacher A, Romorini S, Marini C, Montenegro-Venegas C, Altrock WD, Gundelfinger ED, Fejtova A (2013) Regulation of presynaptic anchoring of the scaffold protein Bassoon by phosphorylation-dependent interaction with 14-3-3 adaptor proteins. *PLoS ONE* 8: e58814

Soriano FX, Chawla S, Skehel P, Hardingham GE (2013) SMRT-mediated co-shuttling enables export of class IIa HDACs independent of their CaM kinase phosphorylation sites. *J Neurochem* 124: 26 – 35

Tsuriel S, Geva R, Zamorano P, Dresbach T, Boeckers T, Gundelfinger ED, Garner CC, Ziv NE (2006) Local sharing as a predominant determinant of synaptic matrix molecular dynamics. *PLoS Biol* 4: e271

Vaithianathan T, Akmentin W, Henry D, Matthews G (2013) The ribbon-associated protein C-terminal-binding protein 1 is not essential for the structure and function of retinal ribbon synapses. *Mol Vis* 19: 917 – 926

Valente C, Luini A, Corda D (2013) Components of the CtBP1/BARS-dependent fission machinery. *Histochem Cell Biol* 140: 407 – 421

Vashishta A, Habas A, Pruunsild P, Zheng JJ, Timmusk T, Hetman M (2009) Nuclear factor of activated T-cells isoform c4 (NFATc4/NFAT3) as a mediator of antiapoptotic transcription in NMDA receptor-stimulated cortical neurons. *J Neurosci* 29: 15331 – 15340

Verger A, Quinlan KG, Crofts LA, Spano S, Corda D, Kable EP, Braet F, Crossley M (2006) Mechanisms directing the nuclear localization of the CtBP family proteins. *Mol Cell Biol* 26: 4882 – 4894

Voskuyl RA, Albus H (1985) Spontaneous epileptiform discharges in hippocampal slices induced by 4-aminopyridine. *Brain Res* 342: 54 – 66

Wiegert JS, Bengtson CP, Bading H (2007) Diffusion and not active transport underlies and limits ERK1/2 synapse-to-nucleus signaling in hippocampal neurons. *J Biol Chem* 282: 29621 – 29633

Wu C, Ramirez A, Cui B, Ding J, Delcroix JD, Valletta JS, Liu JJ, Yang Y, Chu S, Mobley WC (2007) A functional dynein-microtubule network is required for NGF signaling through the Rap1/MAPK pathway. *Traffic* 8: 1503 – 1520

Xiang G, Pan L, Xing W, Zhang L, Huang L, Yu J, Zhang R, Wu J, Cheng J, Zhou Y (2007) Identification of activity-dependent gene expression profiles reveals specific subsets of genes induced by different routes of Ca(2 +) entry in cultured rat cortical neurons. *J Cell Physiol* 212: 126 – 136

Zhai RG, Vardinon-Friedman H, Cases-Langhoff C, Becker B, Gundelfinger ED, Ziv NE, Garner CC (2001) Assembling the presynaptic active zone: a characterization of an active one precursor vesicle. *Neuron* 29: 131 – 143

Zhang Q, Piston DW, Goodman RH (2002) Regulation of corepressor function by nuclear NADH. *Science* 295: 1895 – 1897